81-3

Final Report

A Study of the Salt-Water Intrusion Problem Between Salina, Kansas, and Solomon, Kansas, in the Smoky Hill River Valley

Carl D. McElwee
Tony Severini
Patrick Cobb
Alfred Fleming
Jim Paschetto
Munir Butt
Pam Watson

Kansas Geological Survey, The University of Kansas
Lawrence, Kansas 66044

Prepared for the U.S. Army
Corps of Engineers

June 1981

ABSTRACT

Between Salina and Enterprise, Kansas, the Smoky Hill River picks up a considerable amount of saline water. The result is that the river downstream during low flows may exceed the recommended drinking-water quality standards for chloride. The Smoky Hill and Kansas rivers are important sources of water for several population centers in eastern Kansas. Therefore, this problem has a considerable impact on a significant part of the Kansas population.

The source of the saline water is predominantly from groundwater dissolution of the Hutchinson Salt Member of the Wellington Formation of Permian Age, with smaller amounts coming from disposal of oil field brines. The dissolution of the salt has caused a collapsed zone to occur trending north-south along the present eastern extent of the salt. This collapsed zone forms a briney aquifer called the Wellington aquifer. The brine in the Wellington aquifer flows generally eastward beneath the Smoky Hill Valley and contaminates the alluvial aquifer and river system primarily between New Cambria and Solomon, Kansas.

Considerable geohydrologic information is available about the problem area, although much more is needed before we can put together a detailed picture of the salt-water intrusion problem. The purpose of this project is to gain a better understanding of the intrusion mechanisms and to evaluate the intrusion. Numerical and analytical models will be applied to the system. These models will be applied within the framework of existing data.

In summary, the groundwater modeling of the Wellington aquifer has shown that:

1) The optimum (maximum salt-water reduction with fewest wells) well field configuration of all that we tested is a line of six relief wells spaced

2,000 feet apart, oriented north-south near the existing cottonwood tree well, each well discharging 100 gpm of brine from the Wellington aquifer.

2) The well configuration described in 1) will produce a 12-20% reduction of salt-water leakage from the Wellington aquifer with about a 245-382% increase in fresh-water leakage from the alluvial aquifer into the Wellington aquifer.

3) Some aspects of the model results were fairly sensitive to the input parameters and some effort should be expended to obtain better information before a more detailed model study is instigated or before relief well construction begins. However, the results presented in this study are not expected to be significantly changed. In particular, the percent reduction of salt-water leakage is not as strongly dependent on the model as one might expect. It is not likely that any Wellington aquifer relief well scheme could achieve a 50% volume reduction in salt-water discharge, if the hydraulic conductivity determined by the USGS on a shale core is representative.

The steady-state alluvial models presented in this investigation indicate that the salt water in the Smoky Hill River Valley should be in an unstable condition near the river. This indicates that unstable upconing should be a dominant mechanism for feeding salt water to the river system. The groundwater system does not uniformly discharge to the river system. The unstable upconing should be most pronounced in those reaches where the groundwater system consistently feeds the river system. These areas could be delineated by seepage and salinity surveys.

The time-varying alluvial model shows that the response of the chloride discharge to a flood event can be qualitatively explained by the unstable upconing mechanism. In addition, the time-varying model shows that several years would elapse before significant benefit would be seen in the river system from a Wellington aquifer relief well scheme.

TABLE OF CONTENTS

I. INTRODUCTION TO THE PROJECT

THE SALTWATER INTRUSION PROBLEM

Between Salina and Enterprise, Kansas, the Smoky Hill River picks up a considerable amount of saline water. The result is that the river downstream during low flows may exceed the recommended drinking-water quality standards for chloride. The Smoky Hill and Kansas rivers are important sources of water for several population centers in eastern Kansas. Therefore, this problem has a considerable impact on a significant part of the Kansas population.

The source of the saline water is predominantly from groundwater dissolution of the Hutchinson Salt Member of the Wellington Formation of Permian Age, with smaller amounts coming from disposal of oil-field brines. The dissolution of the salt has caused a collapsed zone to occur trending north-south along the present eastern extent of the salt. This collapsed zone forms a briney aquifer called the Wellington aquifer (Gogel, 1979). The brine in the Wellington aquifer flows generally eastward beneath the Smoky Hill Valley and contaminates the alluvial aquifer and river system primarily between New Cambria and Solomon, Kansas (Gillespie and Hargadine, 1980).

Considerable geohydrologic information is available about the problem area, although much more is needed before we can put together a detailed picture of the saltwater intrusion problem. The purpose of this project is to gain a better understanding of the intrusion mechanisms and to evaluate the intrusion. Numerical and analytical models will be applied to the system. These models will be applied within the framework of existing data. The data for this project will be obtained from the report by Gogel (1979), from the report by Gillespie and Hargadine (1980), and from personal communications with the U.S. Geological Survey, U.S. Army Corps of Engineers, and the Kansas Water Resources Board. No new field data will be generated by this project.

However, this preliminary model study may very well indicate the need for more or different kinds of field data followed by a more detailed model study.

RESEARCH OBJECTIVES AND PROCEDUES

Objectives

The objectives of the project are as follows:

1. To determine the piezometric head distribution in the Wellington aquifer created by a north-south line (or some other scheme) of relief wells across the Smoky Hill River Valley just east of Salina.
2. To test various proposed mechanisms by which the salt water is fed to the river.
3. To see if the qualitative response of the chloride concentration to a flood event can be predicted.
4. To determine the time frame for the river system to clear itself of the extra salt water after the relief wells are installed.

Procedures

The piezometric head change created in the Wellington aquifer by the relief wells will be modeled using a standard artesian two-dimensional numerical model. Appropriate aquifer parameters, boundaries and fluxes will be used insofar as they are known from existing data. We will rely heavily upon the work of Tony Gogel (1979) of the U.S. Geological Survey for data concerning the Wellington aquifer. We will test various numbers and configurations of relief wells to see what plan is most acceptable.

The detailed mechanism by which the salt water gets into the river system is not well known. There are several possibilities including cavity flow, upconing, diffusion, and direct connection. One or two of these mechanisms

may be dominant; however, they all probably occur to some degree. It is hoped that by modeling these various mechanisms we may be able to pick the most likely by its intrusion characteristics. Both numerical and analytical models may be used.

A short discussion of the various mechanisms may be in order. Cavity flow refers to flow through the collapsed zone from areas of high head to areas of lower head. For example, after a flood event, the fresh head far from the river may be considerably higher than normal even though the river stage has declined back to the normal range. It is possible that this head difference could drive brine through the collapsed zone and up under the river. Upconing is a well-known phenomena occurring when fresh water is pumped from a fresh layer overlying a saline layer. For certain well penetrations and pumpages, the saline layer upcones but remains stable. For other penetrations and pumpages, the saline layer breaks through to the well causing salt water to be pumped. A similar thing could be happening in the Smoky Hill Valley. Normal and flood-induced flow to the river system could cause stable or unstable upconing of the saline water. If stable upconing is occurring, then diffusion is the dominant mechanism by which saline water moves to the river. Unstable upconing would cause the saline layer to break through directly to the river. In some localized areas the river may have cut through the alluvium and be in direct connection with the Wellington aquifer. In these areas there will be direct flow from the Wellington aquifer to the river.

The chloride concentration has been measured in the Smoky Hill River during and after various flood events. It is found that after initial dilution the concentration rises above the normal level then slowly declines back to the normal range. We want to see if one or more of the previously

described mechanisms can account for this increase in chloride concentration after a flood event. The numerical and analytical models mentioned in the previous paragraphs will be subjected to a flood event and their chloride concentration responses calculated.

There is a considerable amount of salt water already in the river alluvium. If the intrusion is stopped by relief wells, there will be a transition period while the river system clears itself of the salt water. The models used to carry out the previous work will be utilized to estimate the chloride concentration as a function of time after the relief wells are installed. It should be possible to estimate the percent reduction in salt load carried by the Smoky Hill River.

GROUNDWATER MODELS

Wellington Aquifer Model

The basic equation used to model confined, isotropic, transient groundwater flow is (Freeze and Cherry, 1979):

$$\text{I-1} \qquad \frac{\partial}{\partial x}\left(T \frac{\partial h}{\partial x}\right) + \frac{\partial}{\partial y}\left(T \frac{\partial h}{\partial y}\right) + \frac{Q(x,y,t)}{A} = S \frac{\partial h}{\partial t}$$

where x and y are Cartesian coordinates, T is the transmissivity, Q is a source or sink term representing water flowing in or out of the model by a variety of mechanisms, S is the storage coefficient, t is the time, and h is the hydraulic head. The hydraulic head is defined as:

$$\text{I-2} \qquad h = \frac{p}{\gamma} + z$$

where p is the fluid pressure, γ is the specific weight of the fluid, and z is the elevation of the point where h is being measured. Darcy's Law tells us that water flows from areas of high head to areas of low head in response to a head gradient. Equation I-1 has been averaged in the z direction and thus is a two-dimensional equation.

The parameters T, Q, and S are basic physical quantities describing the aquifer that must be known if we are going to simulate the aquifer. The transmissivity T has units of length squared over time and basically indicates how easily water may flow through the aquifer. For high T values the water will flow more swiftly for a given head gradient than for low T values. Q/A is the amount of water being recharged or discharged to the aquifer per unit area in units of length over time. Q may be due to actual pumping, rainfall recharge, leakage from an aquitard, etc. S is the storage coefficient and finds its physical origin in the elastic properties of the water and aquifer material. S tells us how much water is released in a unit volume of aquifer when the head is lowered one unit.

In addition to knowing equation I-1 and the physical parameters appearing in it, we must have aquifer boundary conditions and an initial condition on the hydraulic head in order to predict what the hydraulic head will look like at some later time. Two types of aquifer boundary conditions are generally encountered. In one type of boundary condition, the hydraulic head is specified. The simplest example of this is a constant-head boundary such as might exist at the edge of a large lake. The other type of boundary condition requires that the flow or flux of water across that boundary be specified. The simplest example of this would be a barrier boundary with no flow; this would occur near the edges of an aquifer where the permeability approaches zero. The initial condition on h is usually obtained by observing the water

levels in a number of piezometers scattered throughout the area of interest. The quality of the initial condition specification obviously depends on the number of piezometers.

Generally, equation I-1 is implemented by introducing a grid system, employing numerical methods, and utilizing a computer for the solution. The complexity of the solution can be appreciated by realizing that equation I-1 can be written for each node point; and it is very common for the number of node points to be numbered in the hundreds. There is an unknown value, the hydraulic head, which must be found for each node point. If N is the number of node points, we see that there are N equations that must be solved for N unknowns.

All of the concepts just outlined will be used in later sections to simulate the Wellington aquifer with a two-dimensional numerical model. At that time a more detailed description of the model and its data input will be given.

Sharp-Interface Models

Traditionally, sharp-interface models have been applied to coastal areas where sea water intrusion is a concern. The earliest such work was done by Ghyben and Herzberg around the turn of the century. Actually salt water and fresh water will mix (they are miscible). Therefore, one might not expect a sharp interface to develop. In fact, the interface is not sharp; but the dispersion zone may be relatively thin in many situations. If the density contrast is significant, gravity forces may keep the fresh and salt waters more or less separated.

There are two rather well-defined schools of thought for modeling groundwater contamination. In one, the concentration of the pollutant is

assumed small enough so that the density of the fluid is relatively uneffected. This is equivalent to ignoring gravity effects. In this case, hydrodynamic dispersion is considered to be the dominant mechanism controlling the movement of the pollutant. In the literature, this is usually referred to as mass transport modeling. The other school considers fluids with densities significantly greater than fresh water. In this case gravity effects may be a dominant factor controlling pollutant movement. In this situation, sharp interface models are usually used. Of course, it is possible theoretically to model the system exactly and consider all these factors simultaneously. However, the model would be extremely complex; and we know of only one that is available. Practically speaking, one must choose between the mass transport models and the sharp-interface models. We know that there is nearly saturated brine in the Wellington aquifer and its density is significantly greater than that of fresh water. For this reason, we have chosen to work with sharp-interface models while realizing their limitations.

Having made the choice to work with sharp-interface models, the situation is still far from simple. The precise mathematical statement of the dynamic behavior of an interface between salt water and fresh water results in a pair of non-linear partial differential equations in terms of h_f and h_s (see Bear, 1979). Even numerical methods experience difficulties achieving a solution in this case. The common method used to overcome this problem is to use vertically averaged heads in the two fluid bodies equivalent to the Dupuit-Forchheimer assumptions (Bear, 1979). Shamir and Dagan (1971) published the pioneering work in solving a vertically averaged numerical solution. A more recent solution for the two-dimensional case has been published by Mercer and others (1980).

The detailed description of the various sharp-interface models and the appropriate input data will be left to later sections of this report. Most of the necessary data and parameters for sharp-interface models are discussed in the section on the Wellington aquifer Model.

II. PROGRESS REPORT OF WELLINGTON AQUIFER MODEL

THEORETICAL DEVELOPMENT OF GROUNDWATER MODEL

Conservation of Mass Equation

Equation I-1 is the basic partial differential equation that describes the flow of groundwater in a two-dimensional, confined, isotropic aquifer. The equation is derived from the application of the conservation of mass principle to the flow of a fluid through an elemental volume of a porous medium. Solving this equation for $\partial h/\partial t$ would provide a method for predicting the future head distribution given the parameters T, Q, S, and the past head distribution. In effect, we could predict what future aquifer conditions would be from the result of some stress (Q) applied to a defined (T, S, and h) aquifer system. When T is anisotropic and/or heterogeneous in the aquifer system, the analytic solution of equation I-1 is somewhat cumbersome; however, its numerical solution can be achieved relatively easily through the use of high speed digital computers.

Numerical Solution to Conservation of Mass Equation

To numerically solve equation I-1 for the entire aquifer, the aquifer is subdivided into small cells by overlaying a grid system on the aquifer. Equation I-1 is solved numerically for each of these cells. It is assumed that conditions (T, S, Q, h) in each cell are continuous in that cell and can be represented by a single value. The value is assigned to a node placed at the center of each cell (node-centered grid). It must be noted that the value assigned to each node must be the average value of the parameter over the cell area. It is also a rule of thumb that the smaller the size of the cells (the finer the grid spacing) the more accurate the final solution.

A finite-difference technique is used to solve equation I-1 for each cell. If it is assumed that the piezometric surface of an aquifer is

relatively smooth between two adjacent cells with respect to space and time, then the gradients $\partial h/\partial x$, $\partial h/\partial y$, $\partial h/\partial t$, $\partial/\partial x(T\ \partial h/\partial x)$, and $\partial/\partial y(T\ \partial h/\partial y)$ can be approximated by the slope of a straight line. The smoother the piezometric surface, the more accurate the finite-difference approximation. Equation I-1 is solved for every cell using the nodal values of h, S, T, and Q of the four adjacent cells and the method of finite-difference to approximate the gradients listed above. Because equation I-1 is solved for every cell, the computational work is enormous for simulating large aquifers, making the use of computers necessary.

Boundary Conditions

Hydrologic boundary conditions affecting the aquifer are simulated in a computer model by placing certain constraints on the grid cells nearest the hydrologic boundary. The boundary conditions usually encountered in numerical modeling of an aquifer system are constant-flux boundaries, constant-gradient boundaries, or constant-head boundaries. A constant-flux boundary is simulated by specifying the parameter Q at the cells that are on or near the constant-flux boundary. A "no-flow" boundary is one special case of a constant-flux boundary and is simulated by coding T=0 at the effected cells. A constant-gradient boundary is simulated by specifying one of the gradients $\partial h/\partial x$, $\partial h/\partial y$ at the affected node. A constant-head boundary is simulated by coding the program to skip over the nodes designated as constant head nodes. In this manner, the constant-head nodes will retain the same value as designated in the initial head distribution throughout the simulation.

Choice of Computer Program

There is a documented abundance of known computer programs that numerically simulate groundwater aquifers. Most of these programs are designed to simulate aquifers under a number of various boundary conditions (constant-head, constant-flux, constant-gradient, no-flow, etc.) for different types of aquifers (artesian, water table, combined artesian and water table, etc.). Although these programs are very versatile, many have not been extensively used and have possible deficiencies or "bugs" that have not been discovered by researchers. To overcome this problem, the U.S. Geological Survey standard two-dimensional computer model (Trescott and others, 1976) was selected to numerically simulate the Wellington aquifer. The USGS two-dimensional model was well documented in 1976 and has been in general use at Reston, Virginia, for almost a decade. The Kansas Geological Survey's Geohydrology Section has used the program successfully in the past and is currently using the same program for the groundwater modeling of the Big Bend area of Kansas.

APPLICATION TO WELLINGTON AQUIFER

Geohydrologic Considerations

The Wellington aquifer, as referred to in this report, consists of the cavernous zones of the evaporite beds in the Wellington Formation between Salina and Solomon, Kansas. The caverns are filled with brine, which is leaking from the Wellington Formation through a confining shale layer into the unconsolidated alluvial Smoky Hill River Valley. Previous studies (Gillespie and Hargadine, 1980; Gogel, 1979) theorized the shale as an important factor in the leakage of the brine. In areas of small shale thickness or fractured zones, substantial amounts of brine are believed to leak into the alluvial

aquifer. In other areas, substantial amounts of fresh water are believed to seep into the Wellington aquifer. The net effect is to create a circulation system of fresh and salt water. In this picture, the Wellington aquifer is a leaky artesian aquifer. The shale layer and any remaining bedrock that can be found between the shale layer and the alluvium acts as a confining bed. Leakage through this confining bed is driven by the vertical hydraulic gradient, which is the difference in head between the Wellington aquifer and the alluvium divided by the thickness of the confining bed. The leakage rate is controlled by the hydraulic conductivity of the shale layer. In areas where cavern collapse has occurred, the hydraulic conductivity of the confining bed may be substantial, providing a conduit for large amounts of brine to leak into the alluvial aquifer. Therefore, the position of these collapse zones is of major importance for a detailed modeling of the Wellington aquifer. However, since a detailed mapping of the collapse zones has not been conducted, it is assumed that leakage is through a continuous confining bed of variable thickness.

To stop the leakage of brine into the Smoky Hill River Valley, the alluvial aquifer and the Wellington aquifer must be in hydrostatic equilibrium; or the equivalent fresh-water head in the Wellinton must be below the alluvial head. To be in hydrostatic equilibrium, the equivalent fresh-water head in the Wellington aquifer must be the same as the head in the alluvial aquifer. To accomplish this, a system of relief wells has been proposed which will lower the head in the Wellington aquifer. The head near a relief well, however, may be significantly lower in the Wellington aquifer than in the alluvial aquifer. De-watering the Wellington aquifer (and the overlying confining bed for that matter) may cause substantial changes in the effective stress in the confining bed causing possible land subsidence

problems. Also, if the equivalent fresh-water head in the Wellington is substantially lower than the alluvial head, fresh water may move down through areas of higher conductivity, causing further solution of salt and anhydrite. This could again lead to land subsidence problems. Therefore, a constraint on the maximum amount of brine to be pumped must be to keep the drawdown in the Wellington aquifer reasonably small.

To simulate the Wellington aquifer, a node centered grid oriented west-east was superimposed on the area between Salina and Solomon. The grid consists of 570 nodes (15 rows, 38 columns) with a constant grid spacing of 2,000 feet. The grid was oriented to conserve computer storage space and the grid spacing was chosen to provide the maximum amount of accuracy, considering the data available while minimizing computer storage required by the data matrices.

The Wellington aquifer between Salina and Solomon is not a closed aquifer system. Gogel (1979) stated that the Wellington aquifer extends both south of Salina along the Smoky Hill River Valley and north of Salina along the Saline River Valley. Therefore, there should be regional fluxes from the Wellington aquifer under these two river valleys which enter the study area on the western border of the aquifer. To simulate this, the perimeter nodes of the aquifer grid were designated as impermeable. The nodes just east of the western boundary under the influence of these regional fluxes were coded as nodes with injection wells - one well per node. The regional flux estimated to be affecting each node was simulated as a constant-flux boundary condition by injecting that estimated flux into the hypothetical injection well. The regional flux was estimated by applying Darcy's Law of groundwater flow to the

perimeter nodes. The flux was calculated as a product of the hydraulic gradient, the node spacing, and a value of transmissivity derived from the model calibration.

In the initial simulation, the only sources of water (inputs into the aquifer) are the regional fluxes of brine simulated by the injection wells and seepage of fresh water from the alluvial aquifer into the Wellington aquifer. The only discharge of water (outputs from the aquifer) is the loss of brine from the Wellington aquifer, through the confining layer into the alluvial aquifer. This amount of fluid lost from the Wellington aquifer has been estimated for the area between New Cambria and Solomon by Gillespie to be between 0.31 and 1.77 ft^3/sec with an average of .77 ft^3/sec. This value will be compared to the simulated leakage values from each of the calibrated models for model verification. In later simulations additional discharge of brine from the Wellington due to relief wells will be considered.

Model Data Preparation

The study area includes the alluvial valley of the Smoky Hill River between Salina and Solomon, Kansas (Fig. II-1). The area was divided both horizontally and vertically using a 2,000-foot grid spacing (Fig. II-2). A total of 570 sub-areas were produced by the intersection of the lines, each being 2,000 feet square. The center of each of these squares is called a node. Each node position carries a value for various parameters either measured, calculated, or estimated. The area is therefore represented by 15 nodes in a north-south direction and by 38 nodes in an east-west direction, a total of 570 nodes. It is on this basis that data is collected and prepared for computer simulation.

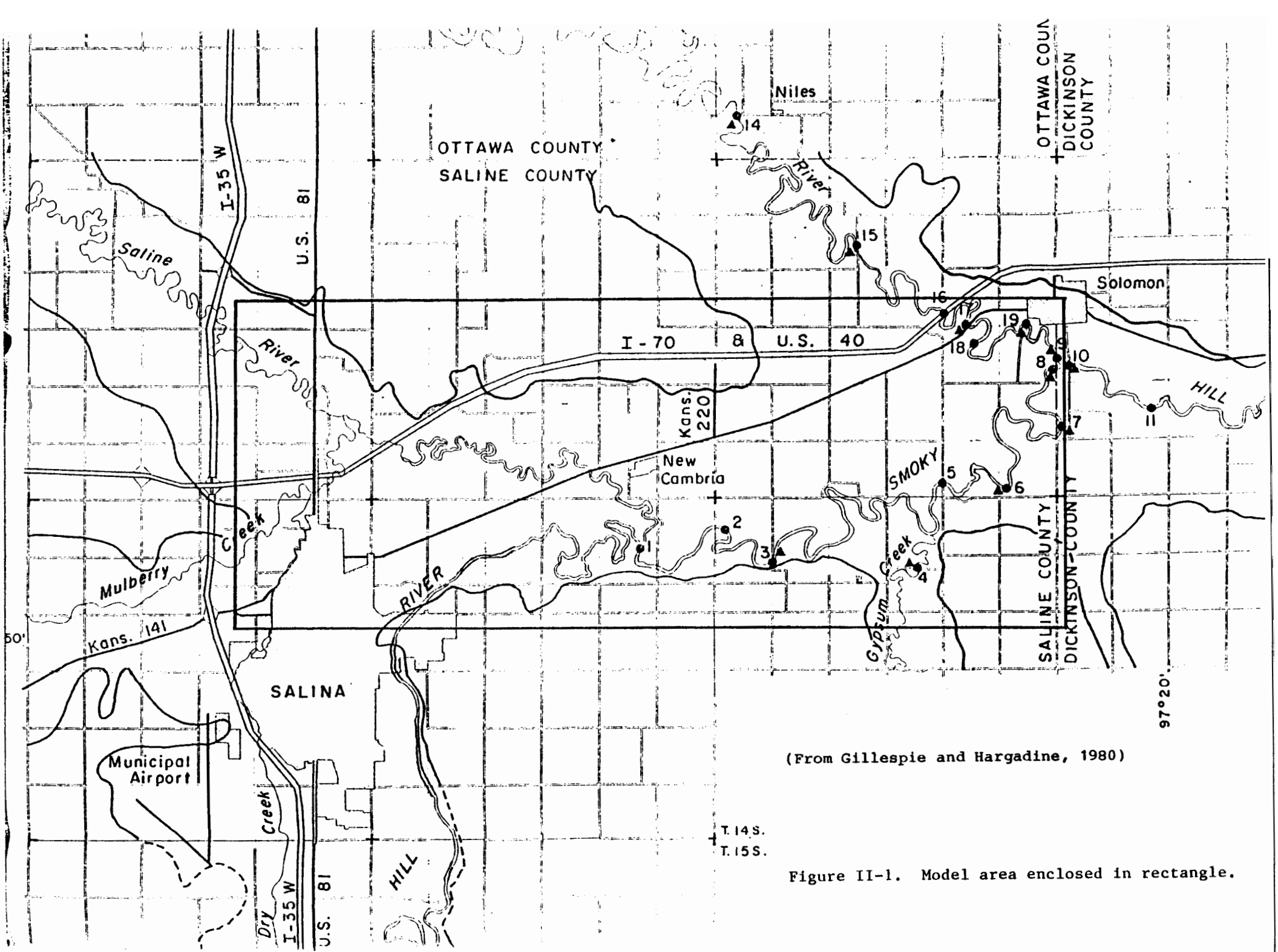

(From Gillespie and Hargadine, 1980)

Figure II-1. Model area enclosed in rectangle.

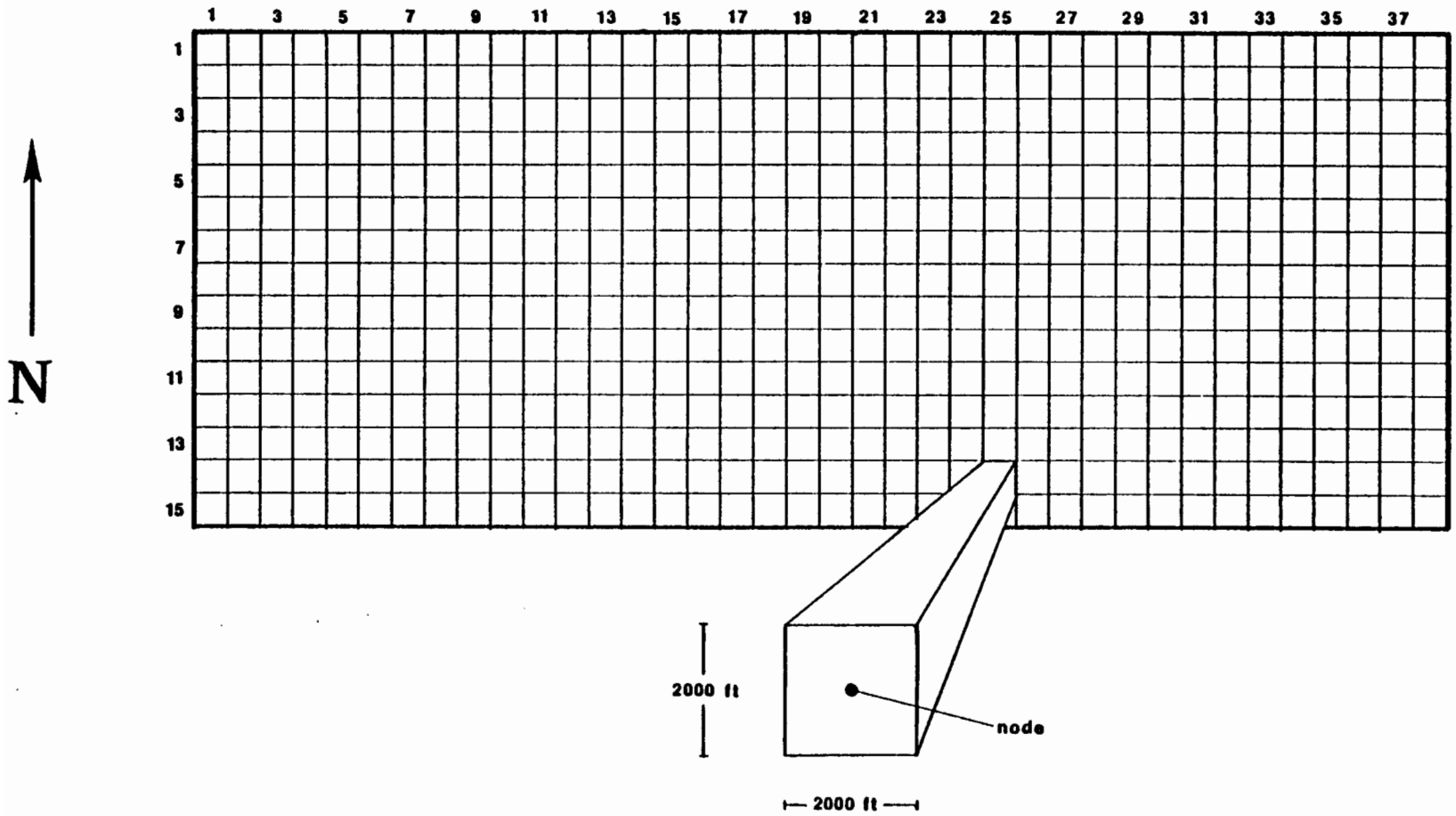

Figure II-2. Illustration of node system.

The condition to be simulated in this part of the study is a leaky aquifer (Wellington aquifer) overlain by an unconfined aquifer (alluvium). The data necessary for simulation of this situation are the transmissivity of the Wellington aquifer, the leakage between the two aquifers, and the initial piezometric surface of the Wellington aquifer. A further discussion of the leakage between the aquifers is in order. From Darcy's Law, the leakage at any node is given by:

$$L = -K \frac{\Delta h}{b} \Delta x \Delta y \qquad \text{II-1}$$

where K is the hydraulic conductivity of the confining bed, b is the thickness of the confining bed, Δh is the head difference between the two aquifers and $\Delta x \Delta y$ represents the area of one grid space (2,000 feet by 2,000 feet in this case). To calculate Δh, we must know the head in the Wellington and the head in the alluvium.

The determination of b in equation II-1 turned out to be rather difficult. The thickness of the confining bed should be given by the difference in the bedrock elevation and the top of the Wellington aquifer. Unfortunately, determining the top of the Wellington Aquifer is rather nebulous. Our first thought was that we would look at all Permian wells in the area and see at what elevation drilling fluid was lost, a cavity was encountered, or gypsum layers were detected. The number of wells drilled into the Permian in recent times for geohydrologic investigations is rather limited. Data on these wells can be found in Gogel (1979) and Gillespie and Hargadine (1980) or by direct communication with those authors. Much more data, somewhat older, was developed by Nick Fent's Hydraulic Drilling Company for the Union Pacific Railroad (Gillespie, personal communication, 1980).

We looked at Fent's test hole logs and selected only those showing evidence of having reached the Wellington aquifer (i.e., loss of circulation, cavity, or gypsum). The number of test holes was so numerous that we restricted our selections to three test holes per mile of UP track. We then determined the elevation of the bottom of the confining bed (or equivalently the top of the Wellington aquifer) and its thickness from the bedrock data. A summary of all the data we developed on the confining bed thickness is contained in Table II-1. Also, a computer map at the scale of the 7½ minute topographic maps is supplied with this report to locate all data points in Table II-1.

The data in Table II-1 are not well distributed over the study area; much of it lies along the UP railroad track that runs from the northeast to the southwest across the area. Also, there is no clear trend of the data. Many times a very thin value will be located near a relatively thick value. Either our method of estimating the confining bed thickness is unreliable or the thickness varies considerably over short distances. In any case, we decided that we could not make a detailed contour map of the confining bed thickness. We did construct a smooth conceptual map of confining bed thickness, which generally thinned to the east.

The leakage is ultimately the thing we must know from equation II-1. We decided to use our conceptual map for b and hide our ignorance in K, the hydraulic conductivity of the confining bed. We shall describe later a procedure by which K is varied in a systematic way to obtain a calibrated model. At that point we can calculate L from equation II-1. It should be emphasized that b is not known in detail so K obtained from the calibration

TABLE II-1. Data on Confining Bed Thickness

Computer Map #	Test Hole or Legal Description	Thickness of Confining Bed (ft.)	Elevation of Bottom of Confining Bed (ft. AMSL)
1	182	24.5	1093.0
2	83	17.0	1106.8
3	85	26.0	1097.2
4	77	22.0	1097.9
5	62	24.5	1085.6
6	81	24.0	1097.9
7	4	18.0	1097.6
8	36	20.0	1100.4
9	45	23.5	1099.1
10	88	16.0	1109.5
11	94	4.0	1113.4
12	96	2.0	1115.2
13	99	9.0	1094.5
14	101	16.0	1103.7
15	104	15.8	1105.4
16	107	19.5	1109.0
17	109	10.0	1107.2
18	110	9.5	1114.5
19	111	25.0	1104.0
20	129	25.0	1103.0
21	119	34.0	1097.5
22	125	32.0	1103.8
23	13-1E-30BDC	19.0	1091.0
24	13-1W-14DAD	3.5	1116.0
25	13-1W-16DCC	17.7	1097.0
26	13-1W-24DDC	1.5	1100.0
27	13-1W-30CCC	2.4	1123.6
28	13-2W-31ADD	33.0	1100.0
29	13-2W-31ADD2	38.0	1093.0
30	13-2W-32CCB	54.5	1083.0
31	13-2W-32CBB2	60.5	1074.5
32	13-2W-32CBB3	15.5	1122.0
33	14-1W-3BBB	19.0	1100.0

procedure will not be directly related to the real physical conductivity. All we know is that we have found a ratio K/b which gives a leakage value that results in a calibrated model.

Discretization of Data

Data matrices necessary for the simulation of the Wellington aquifer are the piezometric surface of the Wellington aquifer, alluvial water table, and thickness of the confining bed. The piezometric surface of the Wellington and the water-table matrices were discretized from contour maps by Gillespie and Hargadine (1980). Node values were determined by linear interpolation between contour lines. It must be noted that the accuracy of the values assigned to each node is dependent upon the accuracy of the placement of the contour lines. The contour lines were positioned according to trends suggested by drilling data that were not very abundant. Therefore, the accuracy of the simulation should not be interpreted as node specific, but rather as indicating general trends of the area.

The thickness of the confining bed matrix was determined by the difference between the elevation of the bedrock and the top of the Wellington aquifer. The elevation of the bedrock was discretized from a contoured bedrock map, also from Gillespie and Hargadine (1980). The elevation of the top of the Wellington aquifer was determined by first contouring the top of the Wellington aquifer (using the procedures outlined in detail earlier) and then discretizing the contours in the method stated above.

Discretization of the contoured data was visually checked for accuracy by comparing input data with contours of the discretized data derived by a computer contouring package at the Kansas Geological Survey Computer Services Section. The data matrices and contours for the piezometric surface of the

Wellington aquifer, the alluvial water table, the bedrock surface, and the saturated thickness of the alluvial aquifer can be found in Figures II-3, II-4, II-5, and II-6 respectively. The node points are shown as small crosses with a numerical value printed close by on the full-size copies of these maps supplied with this report.

Initial Estimates for T and K

We shall describe in the next section a method by which the hydraulic conductivity of the confining bed (K) and the transmissivity of the Wellington aquifer (T) can be determined for a calibrated model. However, it is necessary to have initial estimates for K and T. Gillespie (1979) analyzes some pumping tests and finds T values ranging from 480-7560 ft^2/day and storage coefficient values ranging from .14 to 6 x 10^{-6}. His analysis used simple straight-line techniques to analyze the data and are probably inappropriate over some ranges of the data. A shale core from the confining bed was obtained and analyzed by the U.S. Geological Survey for K. The range of values was 1.2 - 4.4 x 10^{-7} cm/sec. (Gillespie, 1980).

We have analyzed some of the same pumping tests Gillespie used. We have analyzed two drawdown data sets using a program developed at the Kansas Geological Survey (Cobb and others, 1978). This program will analyze pumping tests according to the leaky-aquifer assumption and makes no straight-line approximations. The output from the program is the leakage coefficient (which can be used to calculate K), the transmissivity (T), the storage coefficient (S), and the root-mean-squared error of fitting. The program is not set up to handle recovery data so we could not use all the data Gillespie considered. The first data set was for an observation well 15 feet from the well pumping at 24 gpm. Analysis of this data set gave:

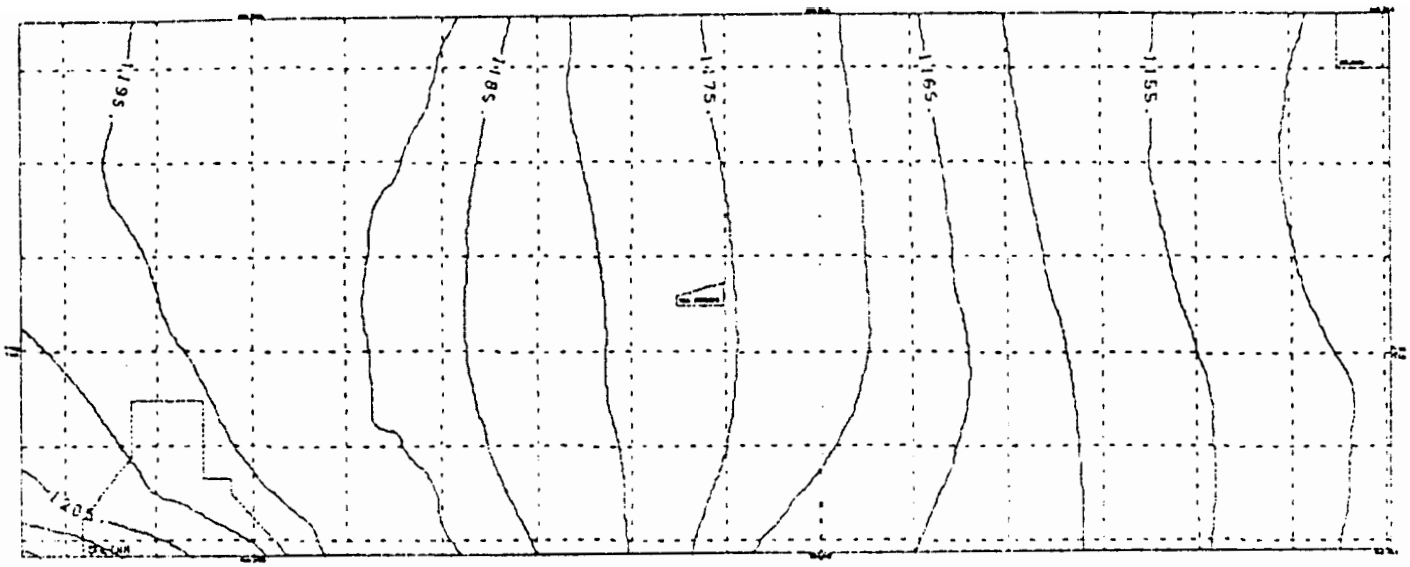

Figure II-3.

CONTOUR MAP OF THE PIEZOMETRIC SURFACE IN THE WELLINGTON AQUIFER

CARL MCELWEE ANTHONY SEVERINI
JIM PASCHETTO AL FLEMING

GEOHYDROLOGY SECTION
KANSAS GEOLOGICAL SURVEY

----1160-----

CONTOUR OF PIEZOMETRIC SURFACE VALUES ARE ELEVATIONS OF PIEZOMETRIC SURFACE IN THE WELLINGTON AQUIFER. COMPUTERIZED CONTOURING BY COMPUTER SERVICE SECTION. CONTOUR INTERVAL IS 5 FEET.

\+

NUMERICAL SIMULATION NODE POSITION

SCALE

1:126,720

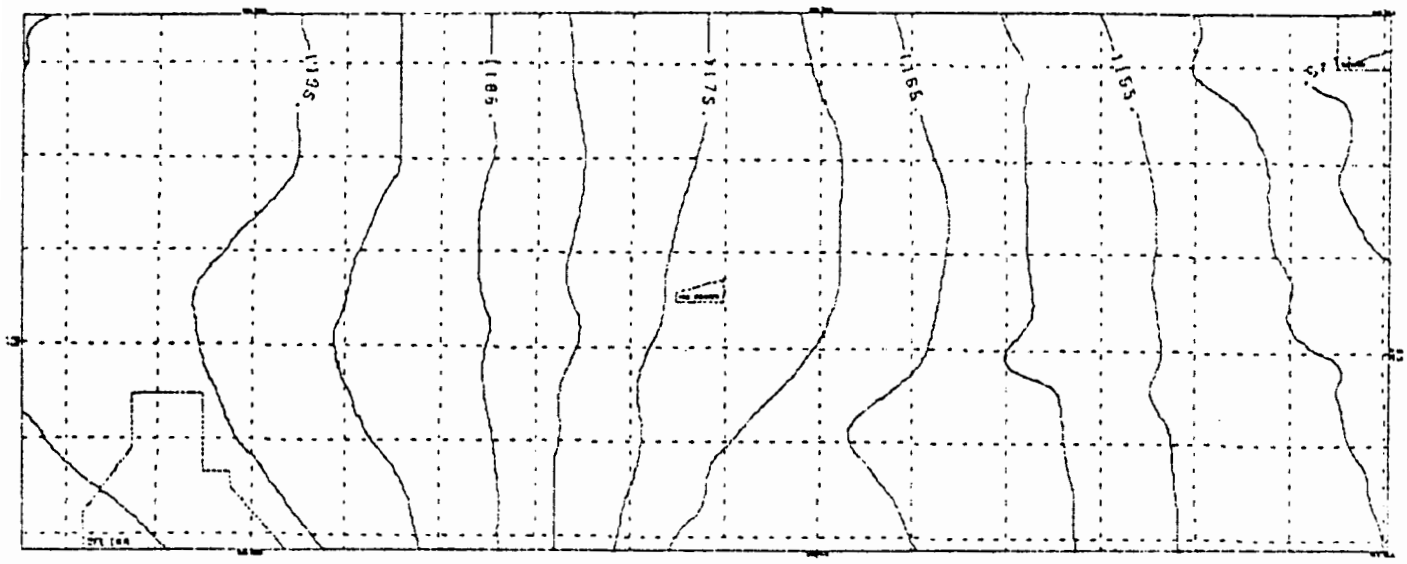

Figure II-4.

CONTOUR MAP OF THE WATER TABLE IN THE SALINA-SOLOMON AREA OF CENTRAL KANSAS

CARL MCELWEE ANTHONY SEVERINI
JIM PASCHETTO AL FLEMING

GEOHYDROLOGY SECTION
KANSAS GEOLOGICAL SURVEY

----1160-----

CONTOUR OF WATER TABLE ELEVATION. VALUES ARE ELEVATIONS OF WATER TABLE IN ALLUVIAL AQUIFER. COMPUTERIZED CONTOURING BY COMPUTER SERVICE SECTION. CONTOUR INTERVAL IS 5 FEET.

\+

NUMERICAL SIMULATION NODE POSITION

SCALE
1:126,720

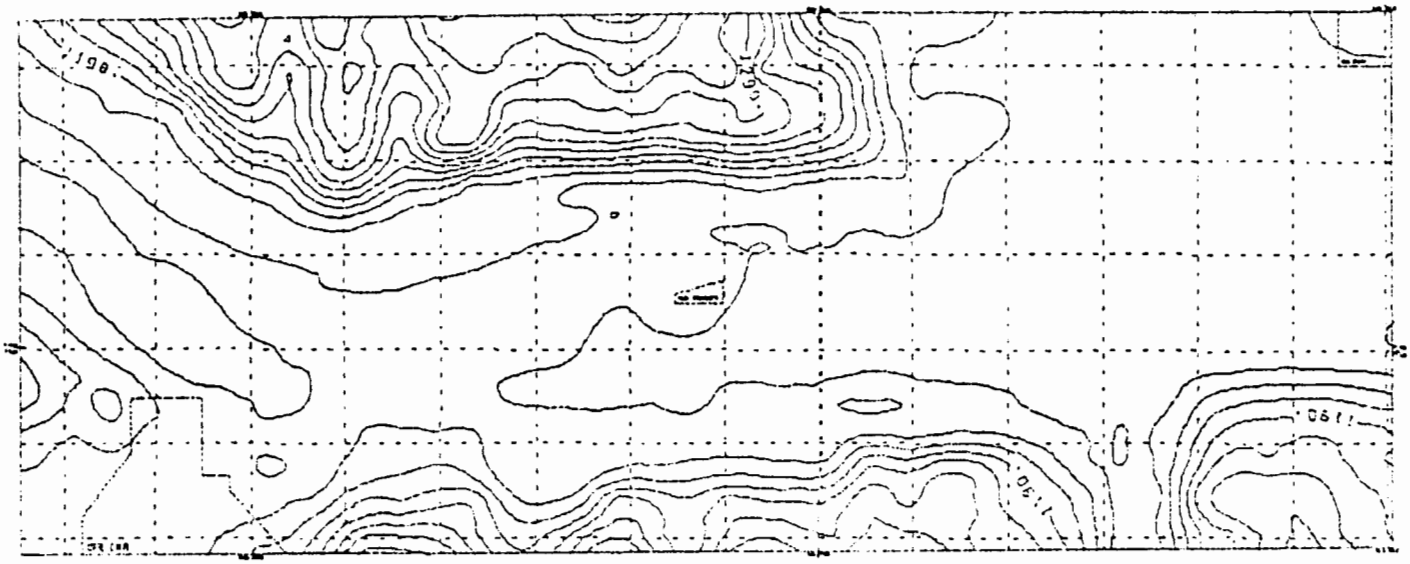

Figure II-5.

BEDROCK CONTOUR MAP IN THE SALINA-SOLOMON AREA OF CENTRAL KANSAS

CARL MCELWEE ANTHONY SEVERINI
JIM PASCHETTO AL FLEMING

GEOHYDROLOGY SECTION
KANSAS GEOLOGICAL SURVEY

----1160-----

CONTOUR OF BEDROCK ELEVATION. VALUES ARE ELEVATIONS OF BEDROCK SURFACE (TOP OF CONFINING BED). COMPUTERIZED CONTOURING BY COMPUTER SERVICE SECTION. CONTOUR INTERVAL IS 20 FEET.

\+

NUMERICAL SIMULATION NODE POSITION

SCALE

1:126,720

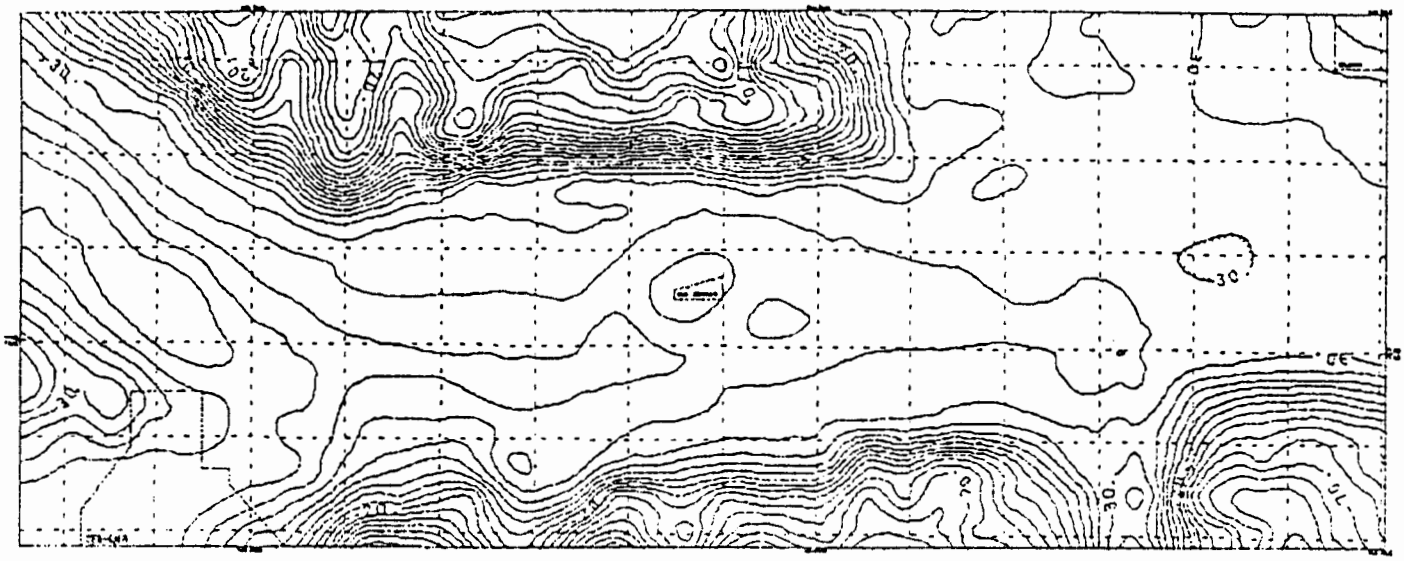

Figure II-6.

SATURATED THICKNESS MAP OF THE ALLUVIAL AQUIFER IN THE SALINA-SOLOMON AREA

CARL MCELWEE ANTHONY SEVERINI
JIM PASCHETTO AL FLEMING

GEOHYDROLOGY SECTION
KANSAS GEOLOGICAL SURVEY

-----100-----

CONTOUR OF SATURATED THICKNESS POSITIVE VALUES INDICATE THE SATURATED THICKNESS OF THE ALLUVIUM IN FEET. COMPUTERIZED CONTOURING BY COMPUTER SERVICE SECTION. CONTOUR INTERVAL IS 10 FEET.

\+

NUMERICAL SIMULATION NODE POSITION

SCALE

1:126,720

$K = 17.9$ ft/day $= 6.3 \times 10^{-3}$ cm/sec

$S = 4.5 \times 10^{-3}$

$T = 1310$ ft^2/day

The other data set was for an observation well at 50.5 feet and it indicated:

$K = .14$ ft/day $= 4.9 \times 10^{-5}$ cm/sec

$S = .56 \times 10^{-3}$

$T = 3412$ ft^2/day

The root-mean-squared error in drawdown for both of these data sets was about .03 feet. This indicates a very good fit of the data to the leaky aquifer equation.

There is quite a bit of variability between the two analyses, but they do fall pretty much in the middle of the range determined by Gillespie. The K values obtained differ by about two orders of magnitude and are considerably greater than those obtained from tests on the shale core. However, the shale core was a small sample and was probably not representative of the secondary permeability that could develop due to slumping and fracturing. If this secondary permeability varied dramatically over short distances (which seems likely), that could explain the two orders of magnitude difference in K determined by the two analyses.

Gillespie and Hargadine (1980) have done some preliminary modeling in this area. They used T of 3000 ft^2/day and K of .00086 ft/day or .086 ft/day depending on whether the confining shale was considered to be intact or not. Because these values fall in the range of values estimated by the pumping tests or core tests, we used them for our initial guesses input to the calibration procedure.

Groundwater Model Calibration by Parameter Adjustment

Models are calibrated when a specific combination of a number of parameters simulate an observed head distribution or a known value of drawdown produced by a known rate of pumpage. The simulation is not unique since an infinite number of combinations of parameters will produce the same simulation. To attain a calibrated model that is an exact replica of the field area would require an enormous amount of extremely accurate data. An objective of this investigation is to determine the final piezometric head distribution caused by the pumping of a network of relief wells. Thus, a calibrated model that accurately simulates the final, steady state position of the piezometric surface of the Wellington aquifer is required.

Since a great deal of emphasis has been placed on the effect of collapse zones in the confining layer by past researchers, four models have been calibrated: one with spatially varying transmissivity and a constant value of hydraulic conductivity of the confining bed; one with a spatially varying hydraulic conductivity of the confining bed and a constant value of transmissivity; and two with a spatially varying transmissivity and hydraulic conductivity of the confining bed. The Wellington aquifer was simulated by all four models to see what inaccuracy in the well-field simulation will be caused by choosing the "wrong" calibrated model. We shall emphasize the well field simulation produced by the models with both spatially varying transmissivity and hydraulic conductivity of the confining bed.

Both models that have only one parameter varying spatially were calibrated for a steady-state simulation of the piezometric head distribution of the Wellington aquifer by a trial-and-error procedure. This procedure

involves the juggling of one parameter, either transmissivity or the hydraulic conductivity of the confining bed, until the initial head distribution is simulated by the computer program.

The third model, the model with spatially varying transmissivity and hydraulic conductivity of the confining bed, was calibrated using a parameter sensitivity procedure developed by Dick Cooley of the U.S. Geological Survey. This method of calibration has just been recently developed and has not been documented. Hence, a brief description of the method is in order.

When calibrating a model, a calculated head distribution, H_n^{Calc}, for all observation (node) points, n, is compared to a known, observed head distribution, H_n^{Obs} for all observation (node) points. If the sum of the difference between the calculated and observed heads is minimal, the model is termed calibrated. Hence, it is possible to define a function, F, such that

$$F = \sum_{n=1}^{N} (H_n^{Obs} - H_n^{Calc})^2 \qquad \text{II-2}$$

where N is the total number of nodes. It is also possible to define a factor, β, that will adjust parameters for model calibration. For the simultaneous adjustment of two parameters, say T and K confined, two multiplication factors are necessary, β_1 and β_2, and the parameter adjustment equations can be written as

$$P_1^{I+1} = (1+\beta_1)\, P_1^I \qquad \text{II-3}$$

$$P_2^{I+1} = (1+\beta_2)\, P_2^I \qquad \text{II-4}$$

or

$$P_k^{I+1} = (1+\beta_k)\, P_k^I \qquad \text{II-5}$$

where P_k^{I+1} is the latest estimate of parameter P_k^I and I is the level of calibration iteration.

Differentiating equation II-2 with respect to β_k we obtain

$$\frac{\partial F}{\partial \beta_k} = \sum_{n=1}^{N} 2(H_n^{Obs} - H_n^{Calc})\left(-\frac{\partial H_n^{Calc}}{\partial \beta_k}\right) \qquad \text{II-5a}$$

For a calibrated model, F is at a minimum. Hence $\partial F/\partial \beta_k = 0$ and equation II-5a becomes

$$0 = \sum_{n=1}^{N} 2(H_n^{Obs} - H_{n(I+1)}^{Calc})\left(-\frac{\partial H_{n(I)}^{Calc}}{\partial \beta_k}\right) \qquad \text{II-5b}$$

where $H_{n(I+1)}^{Calc}$ is the most recently calculated head distribution at the I+1 iteration level of calibration. It is also possible to define $H_{n(I+1)}^{Calc}$ in the following manner

$$H_n^{Calc}(I+1) = H_n^{Calc}(I) + \sum_j \frac{\partial H_n^{Calc_{(I)}}}{\partial \beta_j}\beta_j \qquad \text{II-6}$$

which is a first-order Taylor series approximation. Substituting equation II-6 into equation II-5b we obtain

$$0 = \sum_{n=1}^{N} 2\left(H_n^{Obs} - H_n^{Calc}(I) - \sum_j \frac{\partial H_n^{Calc}(I)}{\partial \beta_j}\beta_j\right)\left(-\frac{\partial H_n^{Calc}(I)}{\partial \beta_k}\right) \qquad \text{II-7}$$

If we set

II-8 $$R_n^I = H_n^{Obs} - H_n^{Calc(I)}$$

II-9 $$S_{nk} = \frac{\partial H_n^{Calc(I)}}{\partial \beta_k}$$

and

II-10 $$S_{nj} = \frac{\partial H_n^{Calc(I)}}{\partial \beta_j}$$

we can substitute equations II-8, II-9, and II-10 into equation II-7 and, after re-arranging terms, we obtain

II-11 $$\sum_{n=1}^{N} \sum_j S_{nk}^I S_{nj}^I \beta_j = \sum_{n=1}^{N} S_{nk}^I R_n^I \qquad k=1,2...$$

If we define two matrices, A and B such that

II-12 $$\sum_{n=1}^{N} S_{nk}^I S_{nj}^I = A_{kj}$$

and

II-13 $$\sum_{n=1}^{N} S_{nk}^I R_n^I = B_k$$

equation II-11 is of the form

II-14 $$\sum_j A_{kj} \beta_j = B_k$$

and can be solved for β_j by a simultaneous equation solving scheme for a linear system of equations.

The matrix multiplication of equation II-14 for two parameters β_1 and β_2 becomes

$$\begin{bmatrix} \left(\sum_{n=1}^{N} \frac{\Delta H_n^{Calc}(I)}{\Delta\beta_1} \frac{\Delta H_n^{Calc}(I)}{\Delta\beta_1}\right) & \left(\sum_{n=1}^{N} \frac{\Delta H_n^{Calc}(I)}{\Delta\beta_1} \frac{\Delta H_n^{Calc}(I)}{\Delta\beta_2}\right) \\ \left(\sum_{n=1}^{N} \frac{\Delta H_n^{Calc}(I)}{\Delta\beta_2} \frac{\Delta H_n^{Calc}(I)}{\Delta\beta_1}\right) & \left(\sum_{n=1}^{N} \frac{\Delta H_n^{Calc}(I)}{\Delta\beta_2} \frac{\Delta H_n^{Calc}(I)}{\Delta\beta_2}\right) \end{bmatrix} \begin{bmatrix} \beta_1(I+1) \\ \beta_2(I+1) \end{bmatrix}$$

II-15

$$= \begin{bmatrix} \left(\sum_{n=1}^{N} \frac{\Delta H_n^{Calc}(I)}{\Delta\beta_1} R_n^I\right) \\ \left(\sum_{n=1}^{N} \frac{\Delta H_n^{Calc}(I)}{\Delta\beta_2} R_n^I\right) \end{bmatrix}$$

where

$$\Delta\beta_j = \beta_j(I+1) - \beta_j(I)$$

Once β_1 and β_2 are determined, the parameters being adjusted for calibration of the model, P_1^I and P_2^I, are modified by equations II-3 and II-4 and a new head distribution is calculated using the modified parameters. If the difference between $H_n^{Calc}(I+1)$ and H_n^{Obs} is too large to be acceptable, the entire process can be repeated.

Results of the above procedure for T and K are illustrated in Figures II-7 and II-8. The maps of the transmissivity (T) distribution and the hydraulic conductivity (K) of the confining bed for the joint calibration show the general areas of the Wellington aquifer where the above procedure was used to calibrate the computer model. Using the calibration procedure described, we

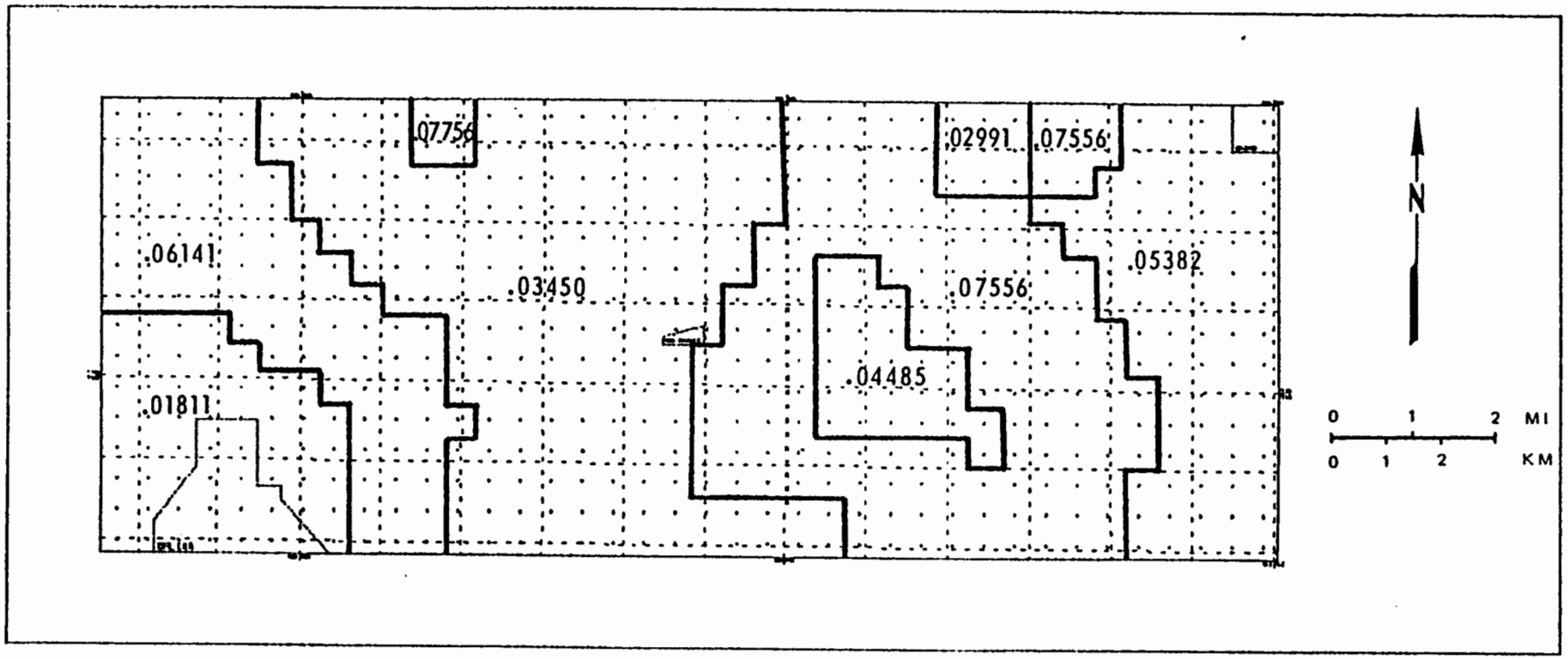

Figure II-7. Transmissivity distribution (ft^2/sec) for the mathematically calibrated model.

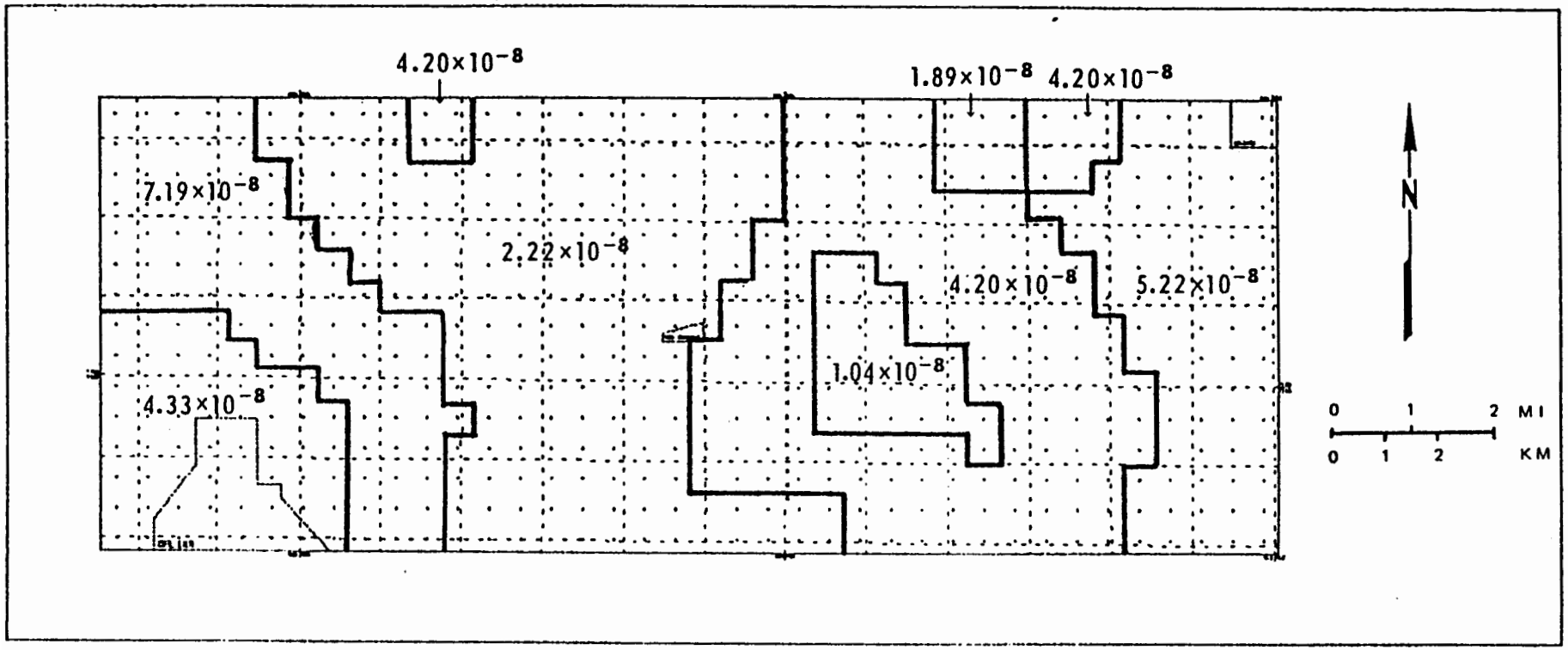

Figure II-8. Confining bed hydraulic conductivity (ft/sec) for the mathematically calibrated model.

were able to match the initial Wellington piezometric surface within about ±2 feet in most places. There were a few isolated spots where the mismatch was somewhat greater.

The mathematical calibration procedure does not allow for intuitive knowledge of the aquifer system. As a result, the mathematically calibrated values of T and S may not show the spatial dependence one had expected. For example, in Figure II-8 some of the higher values of K appear in the western part of the model and in the area of the proposed relief well system. This is to be contrasted with our conceptual model of the confining layer as fairly tight in the western part of the model and fairly permeable in the eastern part due to fractures and collapse.

We decided to "intuitively" calibrate another model to see the effect on final model results. The intuitive model starts out by assuming a low value of K (1×10^{-8} ft/sec) in the western two-thirds of the model and a higher value of K (1×10^{-7} ft/sec) in the eastern third to simulate fractures and collapsed zones. This variation in K is shown in Figure II-9. The transmissivity was then adjusted by trial and error until a match of the steady-state Wellington head was obtained. We were able to match the Wellington head within ± 2 feet. The resulting transmissivity distribution is shown in Figure II-10.

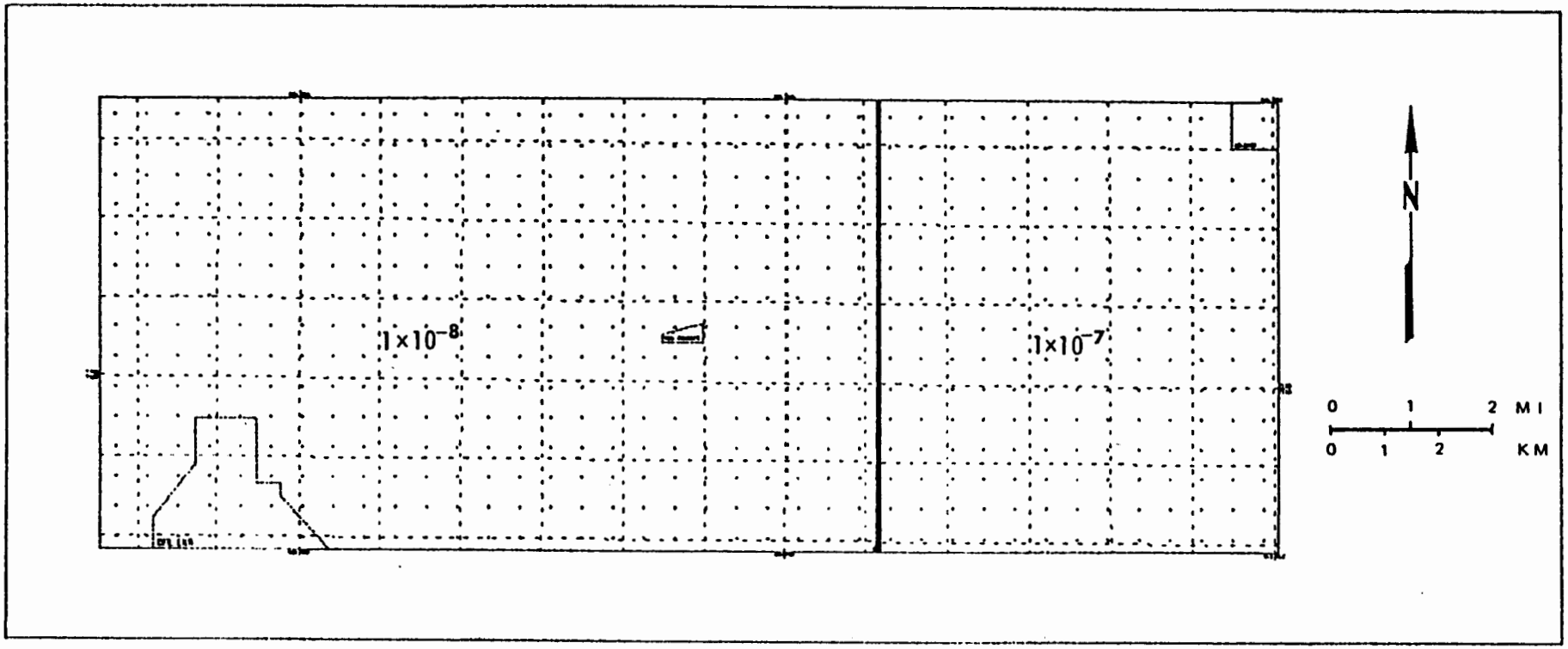

Figure II-9. Confining bed hydraulic conductivity (ft/sec) for the intuitively calibrated model.

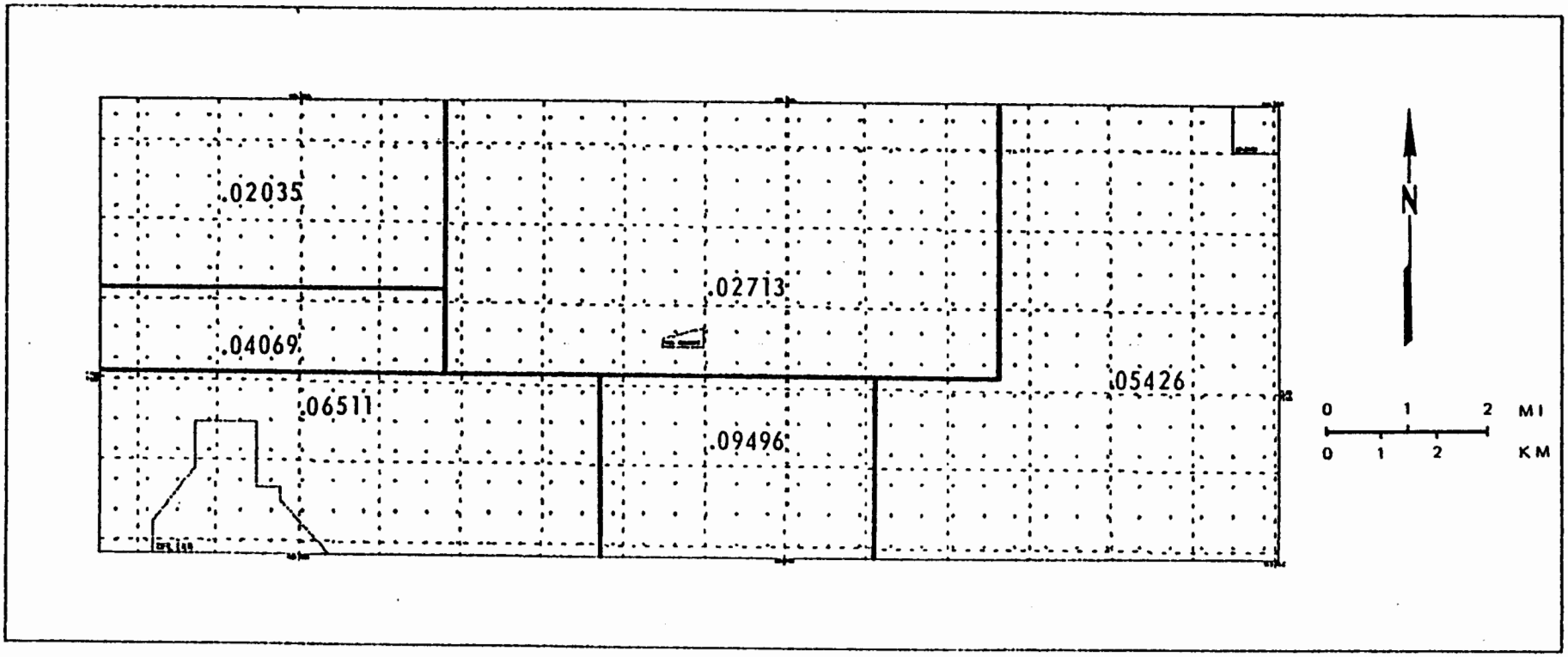

Figure II-10. Transmissivity distribution (ft^2/sec) for the intuitively calibrated model.

WELL FIELD SIMULATION

Well Positions

To simulate the drawdown of a proposed well field, it is necessary to set up the system of constraints that will lower the piezometric head in the Wellington Aquifer to minimize the leakage of brine, minimize any possible dewatering of the Wellington Aquifer, and minimize cost expenditures. Therefore, the distribution of the proposed relief wells has been jointly determined by the Kansas Geological Survey and the U.S. Corps of Engineers.

Preliminary studies were conducted to simulate:

Case I: A single line of six relief wells oriented north-south across the Smoky Hill River Valley near the present cottonwood tree well.

Case II: Three lines of relief wells (20 wells total) oriented north-south. One line positioned as described in Case I and the other two spaced 2,000 and 4,000 feet east of the first line of wells, respectively.

Case III: Three lines of relief wells (20 wells total) oriented as described in Case II but spaced 4,000 and 8,000 feet east of the first line of wells, respectively.

Case IV: One well for every node due east of the well positions described in Case I, spaced 2,000 feet apart (206 wells total).

The node numbers for the wells in the first three cases can be found in Appendix I.

Pumpage Rates

Pumpage rates for the relief wells were selected as those that were both monetarily and physically feasible with equipment commonly used in well construction. The constraints on the maximum pumpage rate was any significant

de-watering of the Wellington aquifer, any significant increase in fresh water leakage into the Wellington aquifer and the monetary cost of brine disposal.

A series of pumpage rates for each well (20, 40, 60, 80, 100 gallons per minute) were tested for Case I. Cases II and III were simulated using a pumpage rate of 22.5 gallons per minute for each well. Case IV was simulated for a pumpage rate of 2.18 gallons per minute for each well. The pumpage rates for Cases II, III, and IV were determined through the equal division among all wells in each case of 450 gallons per minute (1 ft^3/sec); what is believed to be approximately the regional salt-water flux entering the western end of the Wellington aquifer.

To test the sensitivity of the simulation of the Wellington to the parameters, Case I, Test 5 was simulated for all four calibrated models (pumpage rate of 100 gpm for each of the 6 wells). If the results of all four models compare favorably, then the simulation is not very sensitive to T and K. Conversely, if the results of all three models do not compare favorably, then determinations of T and K are extremely important, at least near the well field, in determining the final piezometric surface for any relief well scheme.

Discussion of Results

Results of the Wellington aquifer modeling investigation of this report are summarized in Tables II-2 through II-4. At this point, we must state again that through this investigation we hope to gain insight as to what kind of pumping stress must be placed on the Wellington aquifer to significantly reduce the amount of saltwater leakage out of the Wellington aquifer. Therefore, results should not be regarded as exact, but sufficient to show general trends.

Table II-2. Summary of the simulation results for various pumpage schemes for the mathematically calibrated model.

Case	# of Wells	Well spacing (ft)	Pumpage per well (gal/min)	Maximum drawdown (ft)	Saltwater leakage (ft^3/sec)	% Reduction	Freshwater leakage (ft^3/sec)	%Increase
I test 1	6	2000 NS	20	1-2	1.45	4.0	.67	43.
I test 2	6	2000 NS	40	2-3	1.41	6.6	.90	92.
I test 3	6	2000 NS	60	4-5	1.38	8.6	1.14	143.
I test 4	6	2000 NS	80	5-6	1.35	10.6	1.38	194.
I test 5	6	2000 NS	100	6-7	1.33	12.0	1.62	245.
II	20	2000 NS,EW	22.5	4-5	1.36	9.9	1.32	181.
III	20	2000 NS 4000 EW	22.5	4-5	1.36	9.9	1.32	181.
IV	206	2000 NS,EW	2.18	2-3	1.12	25.9	1.05	123.

Saltwater leakage without pumpage = 1.51 ft^3/sec

Freshwater leakage without pumpage = .47 ft^3/sec

Table II-3. Summary of the simulation results for various pumpage schemes for the intuitively calibrated model.

Case	# of Wells	Well spacing (ft)	Pumpage per well (gal/min)	Maximum drawdown (ft)	Saltwater leakage (ft^3/sec)	% Reduction	Freshwater leakage (ft^3/sec)	%Increase
I test 1	6	200 NS	20	2-3	1.20	9.5	0.43	52
I test 2	6	200 NS	40	5-6	1.14	13.6	0.63	126
I test 3	6	2000 NS	60	9-10	1.11	16.0	0.87	210
I test 4	6	2000 NS	80	12-13	1.08	18.0	1.10	295
I test 5	6	2000 NS	100	15-16	1.05	20.0	1.35	382
II	20	2000 NS,EW	22.5	10-11	1.08	18.3	1.04	270
III	20	2000 NS 4000 EW	22.5	9-10	1.07	19.1	1.03	267
IV	206	2000 NS,EW	2.18	3-4	0.90	31.8	0.83	197

Saltwater leakage without pumpage = 1.32 ft^3/sec

Freshwater leakage without pumpage = 0.28 ft^3/sec

Inspection of Table II-2, for the mathematically calibrated model, reveals that, for all Cases, about 26% reduction of salt-water leakage is the best that can be hoped for and at the expense of a 123% increase in fresh-water leakage (Case IV). However, the cost of constructing 206 relief wells along with the necessary brine disposal system would be prohibitive. More realistic relief well systems (Cases I, II, and III) produce a salt-water leakage reduction of only 4-12% at the expense of 43-245% increase in fresh-water leakage.

The maximum drawdown that occurred at any node point for the various simulations is shown in Tables II-2 through II-4. The maximum drawdown always occurs at a pumping node and is an <u>average</u> value for that node block. The drawdown decreases rather uniformly as one moves away from the relief well system. Contour maps of the drawdown for Case I, test 2 and test 5 are shown in Figures II-11 and II-12 for the mathematically calibrated model.

Table II-3 summarizes the results of the various pumpage schemes for the intuitively calibrated model. About a 32% reduction of salt-water leakage is the maximum that can be obtained in this model for Case IV. The more feasible pumpage schemes (Cases I, II, and III) produce a 9.5-20% reduction of salt-water leakage while causing a 52-382% increase in fresh-water leakage. Contour maps of the drawdown for Case I, test 2 and test 5 are shown in Figures II-13 and II-14 respectively.

All the salt-water leakage reductions shown in Tables II-2 through II-4 are with respect to volumes and not concentrations. We can make some concentration calculations by assuming that all the induced fresh-water leakage moves to the well and is pumped out. For example, in Table II-3 for Case I, test 5, we have 1.35 ft^3/sec of fresh-water leakage; of that, .28 ft^3/sec was present in the original steady state. So the induced fresh-water

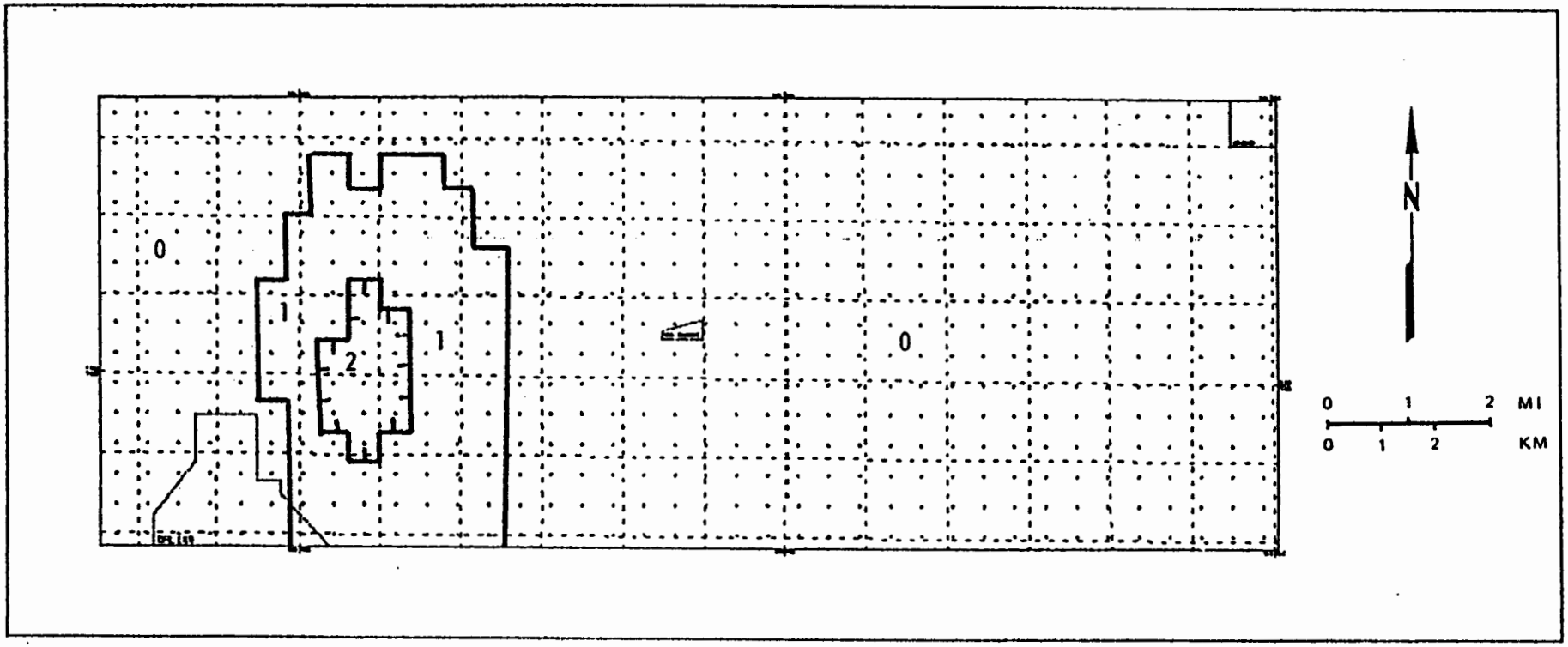

Figure II-11. Drawdown Case I, Test 2 for the mathematically calibrated model.

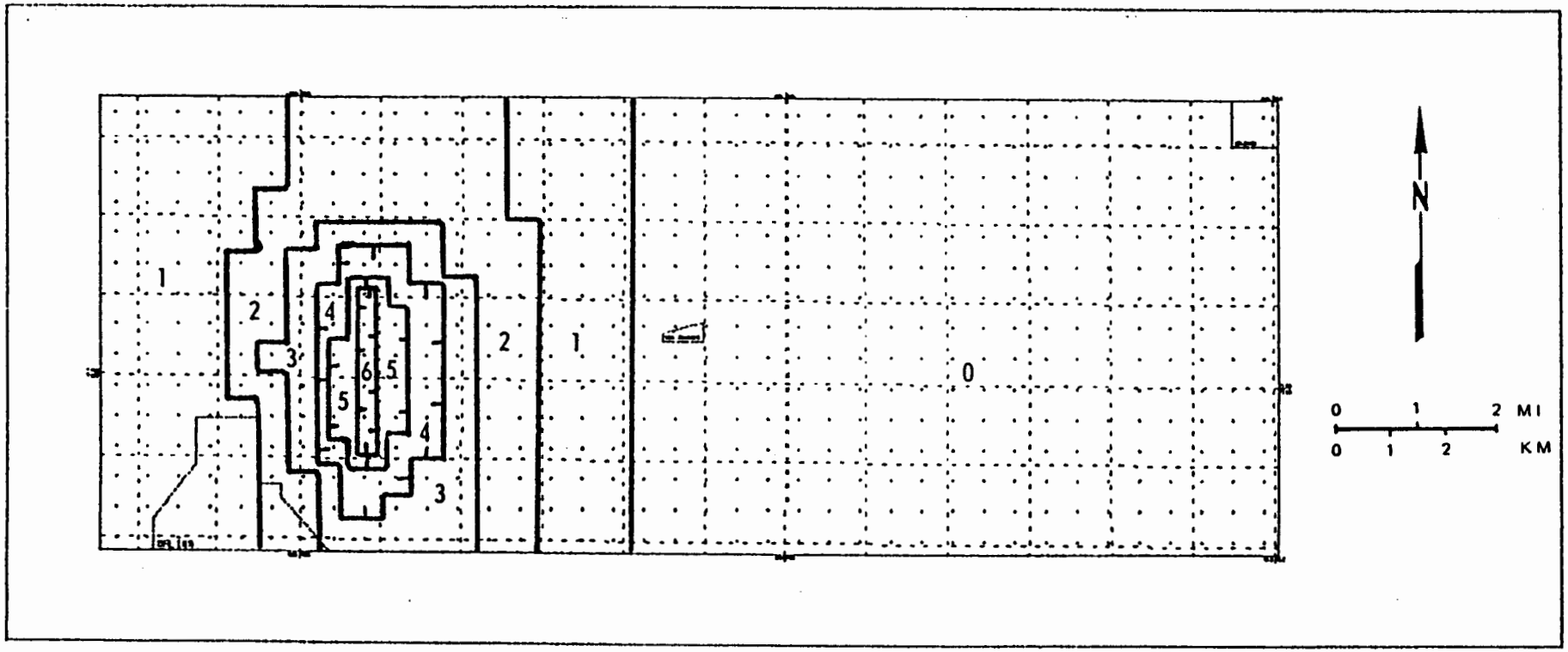

Figure II-12. Drawdown Case I, Test 5 for the mathematically calibrated model.

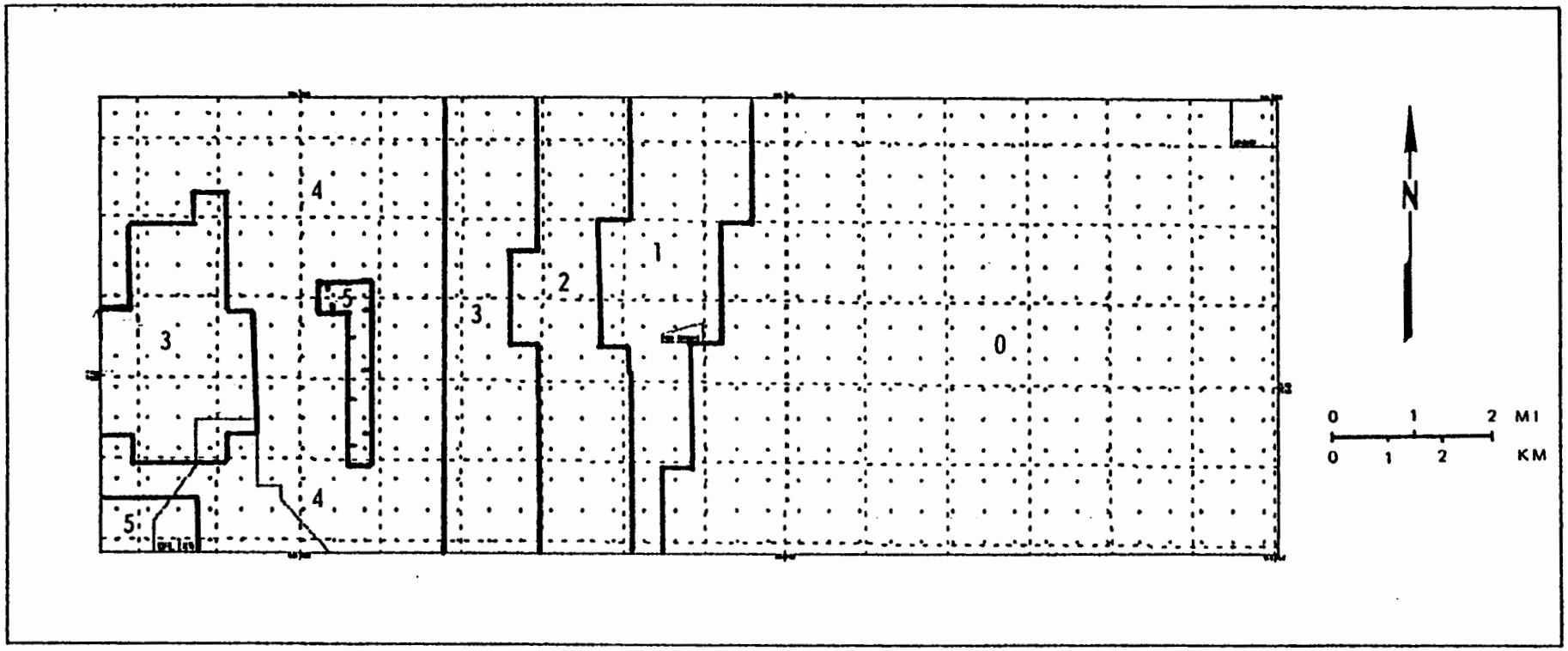

Figure II-13. Drawdown Case I, Test 2 for the intuitively calibrated model.

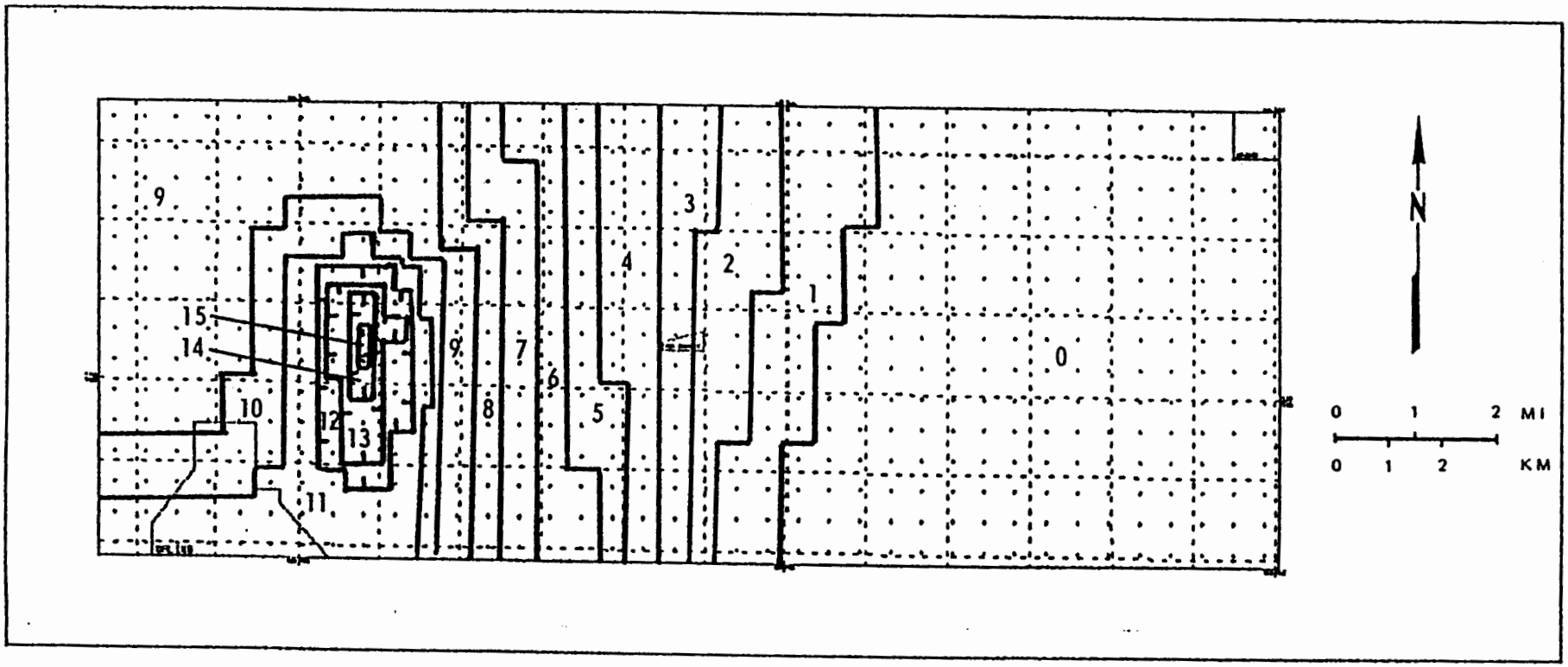

Figure II-14. Drawdown Case I, Test 5 for the intuitively calibrated model.

leakage is 1.07 ft^3/sec. The wells are pumping 1.34 ft^3/sec. If 1.07 ft^3/sec is fresh water, then .27 ft^3/sec must be concentrated brine. Of the original 1.04 ft^3/sec of concentrated brine, this represents about a 26% reduction. Therefore, if the salt-water leakage is expressed as equivalent concentrated brine, we have achieved a 26% reduction. This is to be compared to a 20% reduction in total volume of salt-water leakage. In general, the reduction in terms of equivalent concentrated brine will be a few percent higher than the volume reductions shown in Tables II-2 through II-4 but not radically different.

One question that has not been addressed is whether all the induced fresh-water leakage flows to the well system and is discharged. It seems likely that most does; however, some may flow on to the east in the direction of regional flow and dilute the salt-water leakage somewhat. Examination of this effect could be an area of further study.

Inspection of Table II-4 yields some feel for the sensitivity of model calibrations. The results of the four models calibrated different ways (the first two cases go from one extreme to the other and are not very realistic) show a wide range of possible increase of fresh-water leakage. However, the salt-water leakage reduction varies over a much narrower range of 12-32%. Hence, it is necessary to state that, for a more detailed modeling study and before relief well construction begins, the following parameters should be more closely defined near the well field:

1) Transmissivity of the Wellington aquifer;

2) Hydraulic conductivity of the confining bed;

3) Thickness of the confining bed;

4) Piezometric surface of the Wellington aquifer; and

5) Water table.

Table II-4. Summary of sensitivity of models to T and K.

Case	Maximum Drawdown (ft)	Saltwater Leakage Without Pumpage (ft^3/sec)	Saltwater Leakage With Pumpage (ft^3/sec)	% Reduction	Freshwater Leakage Without Pumpage (ft^3/sec)	Freshwater Leakage With Pumpage (ft^3/sec)	% Increase
K Calibrated T Constant	8-9	1.25	.896	28.3	.212	1.19	461
T Calibrated K Constant	16-17	1.098	.742	32.4	.058	1.04	1690
Mathematically Calibrated	6-7	1.51	1.33	11.9	.47	1.62	245
Intuitively Calibrated	15-16	1.32	1.05	20.5	.28	1.35	382

Number of wells = 6
Distance from adjacent wells = 2000 ft. NS,EW
Pumpage per well = 100 gpm

It also should be pointed out that the value of a 12-20% reduction in salt-water leakage may not be worth the monetary expenditure for the relief-well system.

Conclusions

In summary, the groundwater modeling of the Wellington aquifer has shown that:

1) The optimum (maximum salt-water reduction with fewest wells) well field configuration of all which we tested is a line of six relief wells spaced 2,000 feet apart, oriented north-south near the existing cottonwood tree well, each well discharging 100 gpm of brine from the Wellington aquifer.

2) The well configuration described in 1) will produce a 12-20% reduction of salt-water leakage from the Wellington aquifer with about a 245-382% increase in fresh-water leakage from the alluvial aquifer into the Wellington aquifer.

3) Some aspects of the model results (drawdown, salt-water leakage, and fresh-water leakage) were fairly sensitive to the input parameters and some effort should be expended to obtain better parameter values before a more detailed model study is instigated or before relief well construction begins. However, the results presented here are not expected to be significantly changed. In particular, the transmissivity of the Wellington aquifer the conductivity of the confining bed, and the thickness of the confining bed are the most sensitive parameters. In addition, better definition of the piezometric head in the Wellington aquifer would be beneficial.

The percent reduction of salt-water leakage is not as strongly dependent

on the model as one might expect. Table II-4 shows a variation of 12-32%. It is not likely that any Wellington aquifer relief well scheme could achieve a 50% volume reduction in salt-water discharge if the hydraulic conductivity determined by the USGS on the shale core is representative. If K is an order of magnitude smaller, then significant differences might arise. The effect of mixing by regional water flow to dilute the concentration of the salt-water leakage is something that should be evaluated. However, it seems that about a 50% reduction of actual salt leaked to the alluvium would be an upper limit. This would require that much of the induced fresh-water leakage not flow to the pumping wells but be carried to the natural discharge area.

It should be pointed out that two things that may have a large influence on the feasibility of a relief-well system have not been addressed in this study. First, the presence of collapse features may cause the hydraulic conductivity of the confining bed to be very high locally. It should be determined that no significant collapse features are present near the proposed relief well system. Second, increased fresh-water leakage induced by the relief well system may accelerate natural dissolution and subsidence.

III. PROGRESS REPORT OF SHARP INTERFACE MODELS

THE SALT-WATER UPCONING PROBLEM

The Two Fluid System

If two or more fluids exist as a system, their relationship may range from being miscible in all proportions like water and alcohol, to being totally immiscible like water and oil. Where they are totally immiscible, these fluids will be separated by a discrete surface, and where miscible they will be separated by a zone of dispersion (Hubbert, 1940). In practice, the zone of dispersion is often thin enough relative to the aquifer thickness to be treated by the abrupt interface approximation. This permits the interface to be treated as a material surface, much as the phreatic surface (Bear, 1979). Hubbert points out that between miscible fluids, such as fresh water and salt water, surface tensions are lacking and, hence, no capillary effects are possible except between the fluids and the matrix grains. In most groundwater problems, capillary effects of a fluid-fluid or a fluid-matrix nature are generally ignored. It is also standard practice to ignore the viscosity differences among the various fluids in groundwater work. Verruijt (1980) has recently demonstrated that the velocity distribution along a vertical interface at t=0 is dependent upon $(\mu_1 + \mu_2)/2$ where μ_i is the viscosity of each fluid. Thus, small viscosity differences are justifiably ignored.

Since the system of flow involves two fluids, each fluid must have its own hydraulic head; the values at any point in either region are given by

$$h_1 = z + \frac{p}{\rho_1 g} \qquad \text{III-1}$$

and

III-2 $$h_2 = z + \frac{p}{\rho_2 g}$$

where z is the elevation, p is the pressure, and ρg is the weight density or specific weight.

Conditions for the Existence of an Interface

For a material interface to exist, Hubbert (1940) points out three physical phenomena that must exist. First, each fluid must tend to be driven back into its own realm. Therefore, the hydraulic head of each fluid must increase in the domain of the other. Hence, the normal derivatives must satisfy the following relations.

III-3 $$\left(\frac{\partial h_2}{\partial n_1}\right)_1 > 0$$

III-4 $$\left(\frac{\partial h_1}{\partial n_2}\right)_2 > 0$$

Second, the fluid pressure must be single valued at the interface. Third, the normal component of flow of each fluid at the interface must be zero, i.e.,

III-5 $$\left(\frac{\partial h_1}{\partial n_1}\right) = \left(\frac{\partial h_2}{\partial n_2}\right) = 0$$

Hubbert (1940) has shown that equations III-3 through III-5 imply conditions only satisfied when the lighter fluid overlies the heavier fluid.

The behavior of the interface in relation to the conditions of flow along the interface may be derived by first eliminating p between equations III-1 and III-2, solving for z, and differentiating with respect to S, the path along the interface. The result is

$$\text{III-6} \qquad \sin\Theta = \frac{\partial z}{\partial S} = -\left(\frac{\rho_1}{\rho_2-\rho_1}\frac{\partial h_1}{\partial S} - \frac{\rho_2}{\rho_2-\rho_1}\frac{\partial h_2}{\partial S}\right)$$

where Θ is the slope measured positively upward in the direction of S, and $\frac{\partial h_1}{\partial S}$ and $\frac{\partial h_2}{\partial S}$ are proportional to the velocity of fluids 1 and 2 in the direction S.

If neither fluid is in motion $\sin\Theta = 0$, implying a horizontal interface. If the heavy fluid (ρ_2) is assumed to be static, equation III-6 reduces to

$$\text{III-7} \qquad \sin\Theta = -\frac{\rho_1}{\rho_2-\rho_1}\frac{\partial h_1}{\partial S}$$

As $\frac{\partial h_1}{\partial S}$ increases the interface rises in the direction of flow.

The elevation of any point on the interface may be determined by eliminating p from equations III-1 and III-2 and solving for z:

$$\text{III-8} \qquad z = \frac{\rho_2}{\rho_2-\rho_1} h_2 - \frac{\rho_1}{\rho_2-\rho_1} h_1$$

From equation III-8 it is obvious that for a static fluid 2 (h_2 is constant), the elevation of the interface, z, is dependent upon the value of h_1 at any point on the interface.

Upconing of a Horizontal Interface

For the sake of simplicity let it be assumed that a body of fresh water overlies a body of salt water and that these bodies are separated by a horizontal interface. Now suppose that a sink starts to operate in the fresh water at some distance above the interface. The flow that begins to be

directed toward the sink implies that a change is occurring in the potential field of fluid 1. Equations III-7 and III-8 depict the behavior of the interface as the field values change. As the values of h_1 decrease along the interface, flow develops tangentially along the interface in the direction of decreasing h_1. The interface will rise in the direction of flow as predicted by equation III-7. Equation III-8 corroberates this result. As h_1 decreases on the interface, the second term on the right-hand side of equation III-8 decreases in value and z increases.

The question not answered by equations III-7 and III-8 is whether or not the rise of the interface can continue to the upper limit implied by III-8 without the salt water entering the sink. A stable interface will mean an interface that is at steady state for a given density of salt water and a sink of a given strength. An unstable cone is one that has broken through to the sink. Muskat (1937) addressed the problem by considering the effects of a change in fluid pressure at a point on an oil-water interface, where the water was considered to be in hydrostatic equilibrium. We shall modify his work to consider a two layer system of salt water and freshwater. Thus at any point P(r,z) on the interface

$$P(r,z) + \gamma_S g y = P_b \qquad \text{III-9}$$

where P(r,z) is the fluid pressure, γ_S the specific weight of salt water, y is height of interface above original level, and P_b is the original pressure at the interface at the level of the undisturbed interface far from the sink (Figure III-1). Equation III-9 represents the necessary condition for the cone to remain in a static condition below the sink while flow occurs to it. Physically it means that if at some point P(r,z), the drop in pressure below

Figure III-1. Schematic of a water-coning system in a homogeneous medium

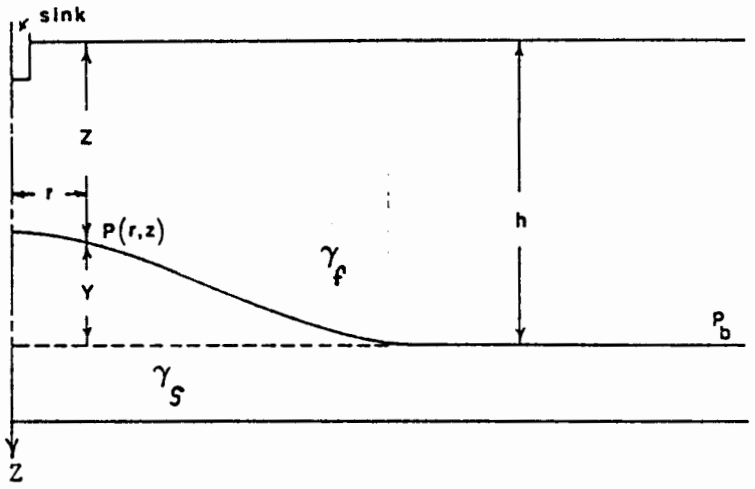

the original pressure can be compensated by a salt water column rising to the height y, static equilibrium will result.

III-10 $$\Delta P(r,z) = gy(\gamma_s - \gamma_f)$$

The convergent flow in the fresh water zone toward the well results in a head gradient that increases rapidly as the well is approached. In the salt water zone we assume a constant hydrostatic head. If equation III-10 is satisfied, we have stable upconing to a height y. If the sink is discharging at too great a rate, equation III-10 cannot be satisfied and the salt water continues moving upward until it reaches the sink. At this point, the sink begins to discharge a mixture of salt water and fresh water. This situation is known as unstable upconing.

In a real physical situation where salt water is overlain by fresh water, a zone of transition will have developed due to hydrodynamic dispersion. Bear (1979) points out that as the salt-water cone rises, this zone widens; and hence, salt water of some lesser concentration may enter the sink even if the calculated sharp interface achieves a stable height. In the following discussions, the assumption of a sharp interface will be used.

Physical Parameters Effecting Upconing

A more detailed analysis of this problem has been done by Bear and Dagan (1964, 1966a, 1966b, 1968) and Schmorak and Mercado (1969). Most of these analyses are to find the height of a stable cone. If unstable upconing occurs the description is much more complex and numerical methods will probably have to be used. They find that a number of factors are important in determining whether stable or unstable upconing occurs. Of course, the greater the sink

discharge, the higher the cone of salt water. For a given physical situation the sink discharge cannot be greater than some maximum value for stable upconing. The penetration of the sink and the depth of interface below the sink are also very important parameters. Obviously, the closer the sink approaches to the interface, the more one approaches unstable upconing. Also the density contrast of the two waters is very important. The denser the salt water, the more stable the situation. In order to address the possibility of upconing in the Smoky Hill River Valley between Salina and Solomon we must have at least some estimate of these and other physical parameters.

The Smoky Hill River is a gaining stream between Salina and Solomon as reported by Gillespie and Hargadine (1980). They report that: "The average gain between the New Cambria gaging station (site 3) and the mouth of the Solomon River (site 8) was 15.6 ft^3/sec." This was the result of four seepage surveys made during periods of near-constant base flow with no recent measurable precipitation. Therefore, this should be a pretty good estimate of the amount of groundwater discharging into the river. The sites are shown by Gillespie and Hargadine (1980) in their Figure 16, part of which is reproduced here as Figure III-2. The stream meanders considerably between sites 3 and 8 and the distance is approximately 16 river miles. The cross-sectional models that we will be using later cannot handle the meandering pattern; they assume a straight river perpendicular to the cross section. For this reason, we measured the distance between sites 3 and 8 as a series of straight-line segments joining sites 3, 5, 6, 7, and 8. The distance between sites 3 and 8 measured this way was approximately 7 miles. The average groundwater discharge to the river per unit length, Q/ℓ, is an important parameter and can now be calculated.

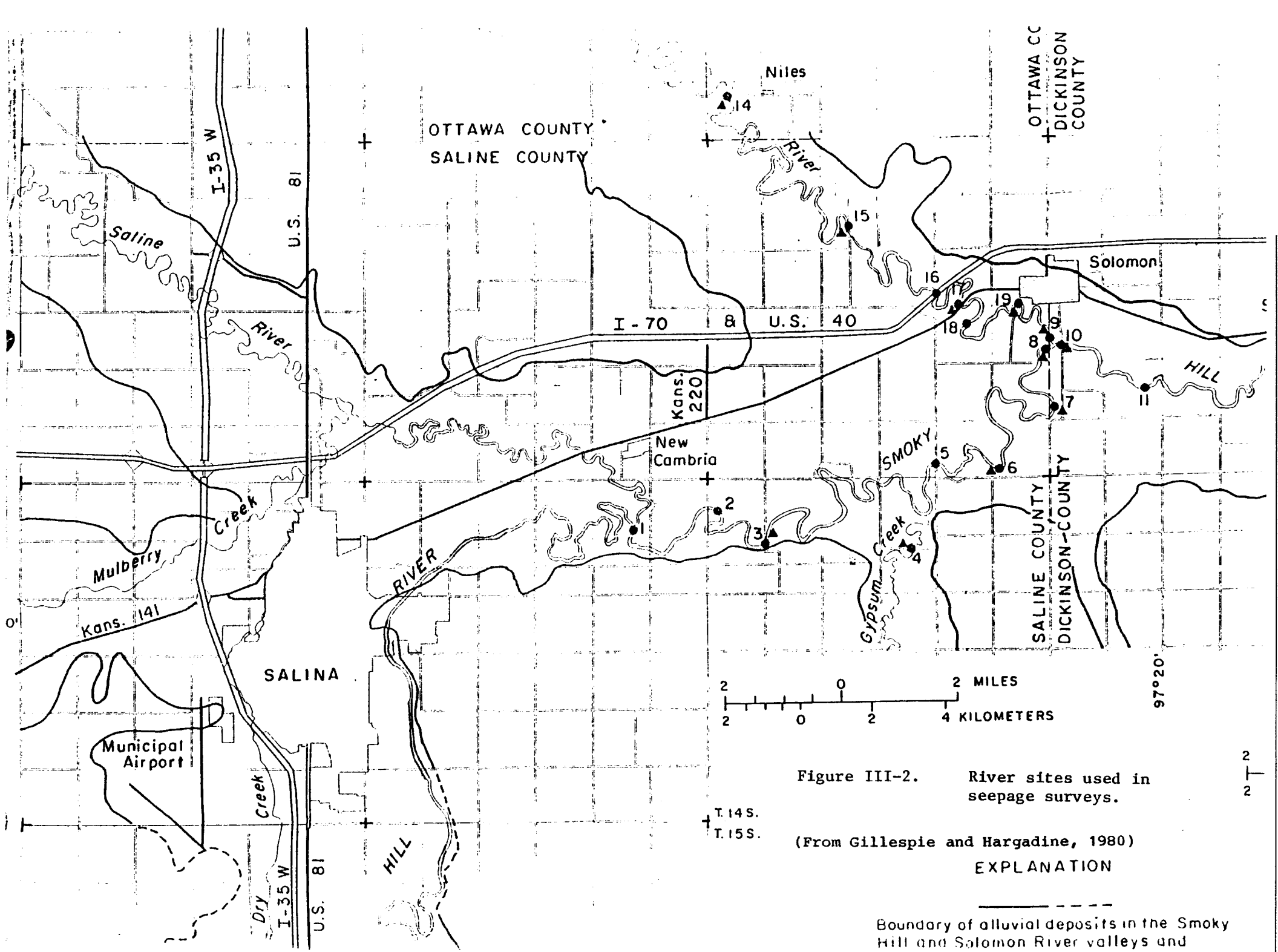

Figure III-2. River sites used in seepage surveys.

(From Gillespie and Hargadine, 1980)

$$Q/\ell = \frac{15.6 \text{ ft}^3/\text{sec}}{7 \times 5280 \text{ ft}} = .000422 \text{ ft}^2/\text{sec}$$

$$= 36.4 \text{ ft}^2/\text{day}$$

A related parameter, the groundwater recharge, R, can also be calculated. Referring to Figure III-2, we see that the average valley width east of Salina is about 3.5 miles. The average recharge can now be calculated.

$$R = \frac{Q/\ell}{3.5 \times 5280 \text{ ft}} = .00197 \text{ ft/day}$$

$$= 8.63 \text{ inches/yr}$$

All three of these parameters - Q/ℓ, average valley width, and recharge - will be used in later sections.

The height of the bottom of the sink or river above the undisturbed salt-water interface is an important parameter as discussed earlier. We do not have good detailed information as to the position of the salt-water interface. However, it is clear that this distance cannot be greater than the saturated alluvial thickness which is shown in Figure III-3. The saturated thickness is in the range of 35 to 50 feet; so we know that the distance between the river bottom and the undisturbed interface must be less than this.

Another important parameter is the density of the salt water in the Wellington Formation. This information was obtained from the USGS data files (Gillespie, personal communication) for wells in this area both in the Wellington and in the base of the alluvium. The plot of density versus chloride concentration is shown in Figure III-4. It is clear that water ranging from a density of 1.2 to 1.01 is readily available. The fact that water of such varying densities can be obtained would argue against using a sharp interface approximation. However, a model that tried to describe the

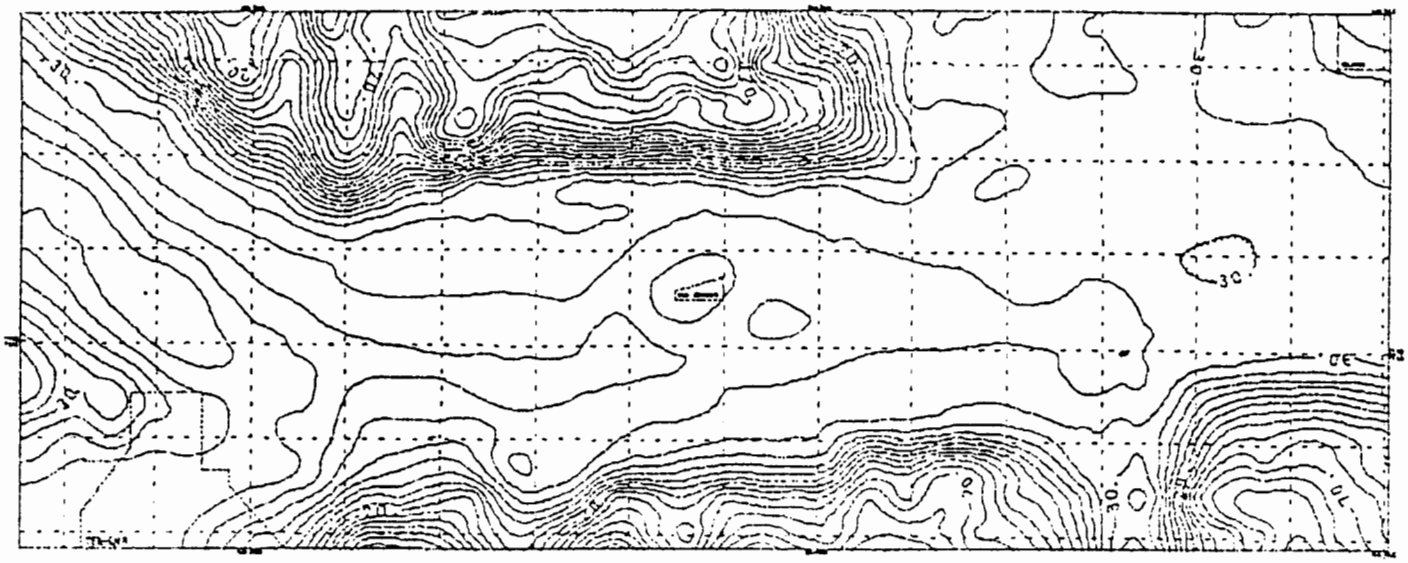

Figure III-3.

SATURATED THICKNESS MAP OF THE ALLUVIAL AQUIFER IN THE SALINA-SOLOMON AREA

CARL MCELWEE ANTHONY SEVERINI
JIM PASCHETTO AL FLEMING

GEOHYDROLOGY SECTION
KANSAS GEOLOGICAL SURVEY

-----100-----

CONTOUR OF SATURATED THICKNESS POSITIVE VALUES INDICATE THE SATURATED THICKNESS OF THE ALLUVIUM IN FEET. COMPUTERIZED CONTOURING BY COMPUTER SERVICE SECTION. CONTOUR INTERVAL IS 10 FEET.

\+

NUMERICAL SIMULATION NODE POSITION

SCALE

1:126,720

Figure III-4. Plot of density versus chloride concentration.

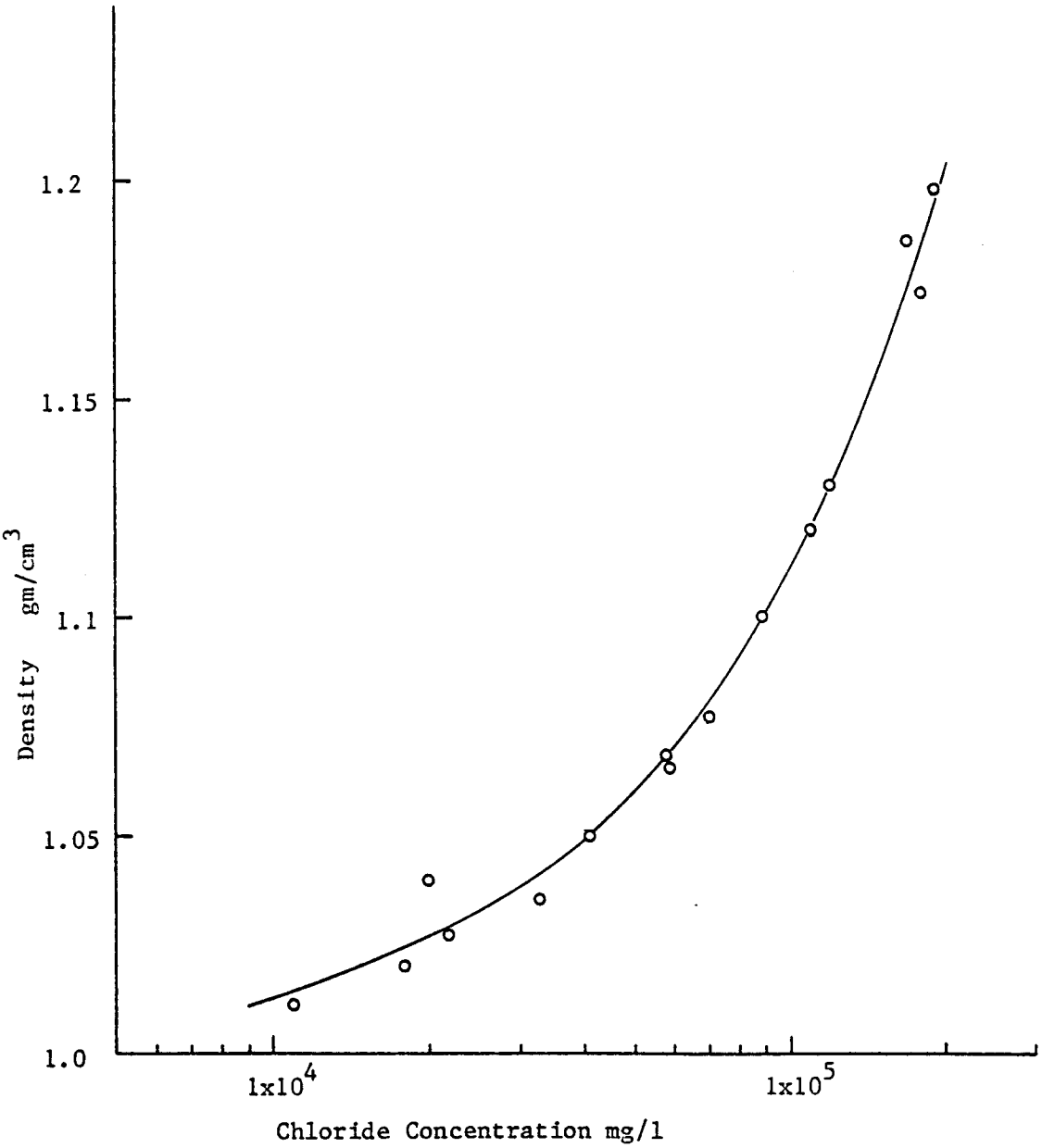

dispersion in detail would be very complex. We feel that much can be learned about the problem by using the sharp-interface approximation.

THE McWHORTER APPROXIMATION

Introduction

In order to predict the hydrodynamic upconing effect of tile drains placed in known fresh-water aquifers underlain by salt water, McWhorter (1972) devised an analytical solution to the problem. For the purposes of this study, it was felt that the physical situation near a horizontal tile drain approximates the drainage of an aquifer by the base flow contribution to an effluent stream such as the Smoky Hill River.

In McWhorter's depiction of flow toward a drain, as shown in Figure III-5a, the drain of radius a is centered a distance D below a water table, in a fresh-water system of thickness m, defined by the free surface and the undisturbed interface. The system is to reach a steady state, with the free surface in the drain being a distance d above the undisturbed interface and a constant head at x=L providing the fluid to the system. The interface is assumed to be stable. The approximations in transferring the concept to the natural stream are the assumptions of drain size and of actual maintenance of the constant-head boundary at distance x=L. If a large body of subsurface storage is available, this constant-head condition may be approximated for certain time periods. If recharge is sufficient to supply just the discharge prescribed by the gradient to the stream, this condition may be a good approximation.

In order to cast the problem into a form more convenient for analysis, McWhorter (1972) recognized that, in most instances of interest, $D < d$ and hence "the contribution to the drain discharge due to flow above the drain

Figure III-5. McWhorter's Approximation

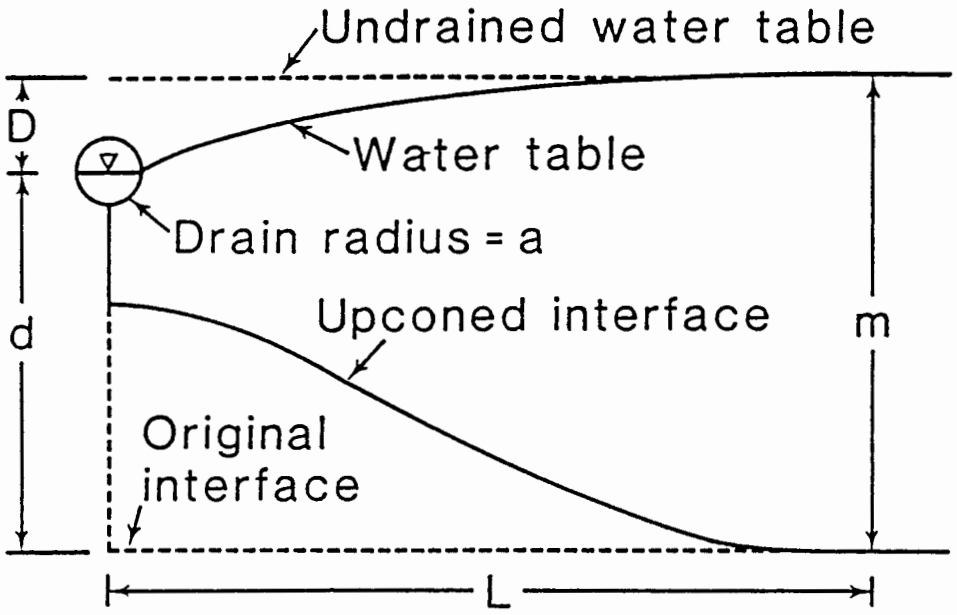

a. Flow toward a drain

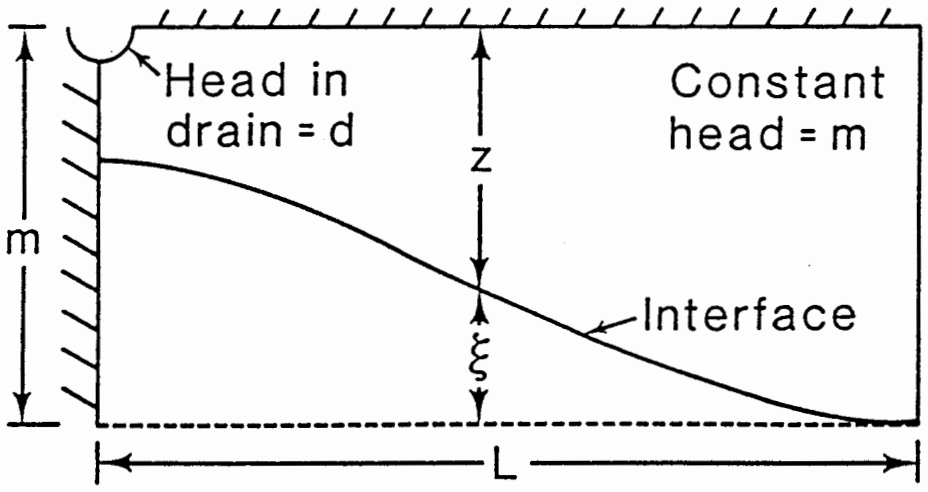

b. Idealized flow toward a drain

(after McWhorter, 1972)

elevation is small compared to that from below the drain." This essentially reduces the problem to that of a confined aquifer of thickness m (see Fig. III-5b) drained by a line sink of constant strength at x=0, z=0 (x measured positive to the right and z measured positively downward, relative to the location of the sink). A solution to the upconing problem is obtained by assuming that the interface does not effect the distribution of head in the fresh-water region. This is essentially the same approximation invoked by Muskat and Wyckoff (1935) in their study of the upconing problem in oil reservoirs. In order for this assumption to approximate reality the change in elevation of the cone must remain small. Muskat (1937) indicates in regard to this approximation that the quantitative details will be effected, but the general features of the critical height of the cone are still valid. McWhorter points out that his approximation predicts a higher discharge than could actually be expected for any particular position of the interface.

Mathematical Equations

McWhorter (1972) derived an approximate distribution for head in a system defined by Figure III-5b using the method of images (Cobb, 1980). The unperturbed fresh water head distribution is approximately:

$$\text{III-11} \qquad H_f(x,z) = \frac{Q}{2\pi K_f} \cdot \ln\left\{\cosh\frac{\pi x}{m} - \cos\frac{\pi z}{m}\right\} + \text{constant}$$

He points out that for this distribution, if $L > d$, $H_f = m$ at $x=L$. Subject to the boundary conditions $H_f = m$ at $x=L$ and $H_f = d$ on $x^2+z^2=a^2$ (see Cobb 1980 for details), it is shown that the discharge to the drain is given by

$$\text{III-12} \qquad Q = 2\pi K_f(m-d)/\ln\left\{\frac{\cosh\frac{\pi L}{m} - 1}{\cosh\frac{\pi a}{m} - 1}\right\}$$

and the head distribution by

$$\text{III-13} \qquad H_f = \frac{Q}{2\pi K_f} \bullet \ln\left\{\frac{\cosh\frac{\pi x}{m} - \cos\frac{\pi z}{m}}{\cosh\frac{\pi L}{m} - 1}\right\} + m$$

Finally, the position of the perturbed interface, relative to its original position is given by

$$\text{III-14} \qquad \xi = \frac{\gamma_f}{\Delta\gamma}(m - H_f^i) \quad , \quad \Delta\gamma = \gamma_s - \gamma_f$$

Using the relationship $z = m - \xi$ derived from Figure III-5b, equation III-13 may be recast to the form

$$\text{III-15} \qquad H_f^i = \frac{Q}{2\pi K_f} \bullet \ln\left\{\frac{\cosh\frac{\pi x}{m} - \cos\pi\left(1 - \frac{\xi}{m}\right)}{\cosh\frac{\pi L}{m} - 1}\right\} + m$$

on the interface. Simultaneous solution of equations III-14 and III-15 are used to determine the position of the interface ξ and the free surface H_f^i. McWhorter (1972) used these equations to derive the maximum safe installation depth D for a tile drain to avoid upconing for a given discharge. The equations were used in a slightly different strategy for this investigation.

Graphical Solution

In order to easily determine the stability of a cone of saline water, a graphical solution of equations III-14 and III-15 is convenient. Some preliminary simplification is possible on equation III-15. As McWhorter points out, stability of the cone at the point directly beneath the stream implies stability of the entire cone. Thus, solution at x=0 is an appropriate indicator for the system. Since cosh 0 = 1, equation III-15 reduces to:

$$\text{III-16} \qquad H_f^i = \frac{Q}{2\pi K_f} \bullet \ln\left\{\frac{1 - \cos \pi\left(1 - \frac{\xi}{m}\right)}{\cosh \frac{\pi L}{m} - 1}\right\} + m$$

Now equation III-14 can easily be manipulated to the form:

$$\text{III-17} \qquad \frac{H_f^i - d}{m - d} = 1 - \left(\frac{m}{m - d}\right)\left(\frac{\Delta\gamma}{\gamma_f}\right)\left(\frac{\xi}{m}\right)$$

McWhorter then indicates that after substitution of equation III-12 into equation III-16, some algebraic manipulation leads to

$$\text{III-18} \qquad \frac{H_f^i - d}{m - d} = 1 - \left[\ln\left\{\frac{1 - \cos \pi\left(1 - \frac{\xi}{m}\right)}{\cosh \frac{\pi L}{m} - 1}\right\} \Big/ \ln\left\{\frac{\cosh \frac{\pi a}{m} - 1}{\cosh \frac{\pi L}{m} - 1}\right\}\right]$$

Equations III-17 and III-18 are dimensionless functions in terms of H_f^i and ξ for any set of physical parameters a, m, d, γ_s, γ_f, and L. For a graphical solution, using the argument ξ/m, solving III-18 for a set of physical parameters gives a single curve. The quantity ξ/m is the ratio of the stable cone height to the fresh-water thickness. Solution of equation III-17 for a range of γ_s, again using ξ/m as argument, produces a family of straight lines that may intersect the locus of equation III-18. The possible solutions are (McWhorter, 1972): no intersection, which implies unstable upconing; a tangent to the curve, which implies the critical height for the cone; a non-tangent intersection, which implies a stable cone height. This last situation offers one ambiguity in that two points of intersection may occur for the larger values of ξ/m where the radius of curvature decreases. Muskat and Wyckoff (1935) point out that, in this case, choice of the correct root is dictated by the requirement that the stable free surface represent the lowest potential energy, a condition that is satisifed by the lower cone.

More discussion of the solution will occur when the actual physical problem in the Smoky Hill River Valley is addressed.

Final Transformation of the Approximation

Physical conditions in a natural drainage system of the scale of the Smoky Hill River Valley are such that $L > m > a$. This allows some simplification of the final equations to be made.

First, recall that in its exponential form

$$\text{III-19} \qquad \cosh x = \frac{e^{x} + e^{-x}}{2}$$

Now consider equation III-12, and note that the term

$$\text{III-20} \qquad \ln(\cosh \frac{\pi L}{m} - 1)$$

may be reduced in the following fashion.

$$\text{III-21} \qquad \ln(\cosh \frac{\pi L}{m} - 1) \approx \ln(\cosh \frac{\pi L}{m}) \ , \quad L > m$$

For large L, $\exp[\frac{-\pi L}{m}] \to 0$. This leaves

$$\text{III-22} \qquad \ln(\cosh \frac{\pi L}{m} - 1) \approx \frac{\pi L}{m} - \ln 2$$

Equation III-12 now becomes

$$\text{III-23} \qquad Q \approx 2\pi K_f (m - d)/[\frac{\pi L}{m} - \ln 2 - \ln(\cosh \frac{\pi a}{m} - 1)]$$

or, for the condition $L > m > a$, since one can ignore the log terms

III-24 $$Q \approx 2K_f m\left(\frac{m-d}{L}\right)$$

which approximates the discharge per unit length of a confined aquifer to a stream for both sides.

Equation III-18 must also be modified to reflect the orders of magnitude of the system parameters. Similar approximations applied to that equation yield

III-25 $$\frac{H_f^i - d}{m - d} \approx 1 - \frac{\ln\left[1 - \cos\ \pi\left(1 - \frac{\xi}{m}\right)\right] - \frac{\pi L}{m} + \ln 2}{\ln\left(\cosh \frac{\pi a}{m} - 1\right) - \frac{\pi L}{m} + \ln 2}$$

Equations III-17 and III-25 were solved graphically with the aid of two simple computer programs. The results will be discussed, as well as the effects of varying certain parameters in the next section.

Application to the Smoky Hill River Valley

In order to apply the McWhorter Approximation to the Smoky Hill River Valley, it was necessary to determine the semicircular channel radius, a, characteristic of the average flow of the stream. In order to do this, flow measurements bracketing the average long-term average stream discharge at New Cambria were examined. The value of a was determined to be about 15 feet, and this value was used for all subsequent computations. The results are not too sensitive to the exact value of a.

The average valley half width, L, over the reach of interest is estimated to be 9240 feet. This value was used, along with multiples of 1.50 and 0.66 times that value, in solving the McWhorter equations. Values of m were

selected ranging from 90 to 150 feet, in increments of 10 feet. Values of d, the head value at the stream, were computed for values of L and m by solving equation III-24 for Q=36.4 ft^2/day.

Results of the stability computations for K_f of 50 ft/day are tabulated in Table III-1 for the choices of L and m for fixed a and Q. In general, stable salt-water interfaces become more frequent with decreasing valley width, increasing salt-water density, and increasing fresh-water thickness m. It is noteworthy that the stable configurations involve fresh-water thicknesses much in excess of the 35 to 50 feet of the unconsolidated fresh-water aquifer known to exist over the reach of the Smoky Hill River Valley being studied. Because of this, it is concluded that, in the study area, salt water known to exist in the basal alluvial aquifer is probably in a condition of unstable upconing.

STEADY-STATE INTERFACE CROSS-SECTIONAL MODEL

Introduction

The problem of stable or unstable upconing beneath a gaining stream was addressed in the previous section by use of an analytical approximation called the McWhorter Approximation. The assumption that the upconing salt water does not affect the distribution of fresh-water head will obviously cause some discrepancy between real and approximate upconing stability conditions. An alternative method considers vertically averaged heads in the fresh water and salt-water layers. This method has its own shortcomings for, although it assumes a free surface for the fresh water and accounts for the effect of the rising cone of salt water on the fresh-water head, it ignores the radial convergence of flow under the stream, since horizontal flow is assumed in the z-averaging scheme. Thus, the results of the McWhorter approximation are not

directly comparable to the results of vertically averaged models. The two sets of results may be useful, however, in defining the probable range of water density and stream gain for stable or unstable upconing.

The steady state interface model outlined here is a numerical solution of basic flow equations. It assumes a static body of salt water overlain by a dynamic body of fresh water in which the equipotentials are vertical (horizontal flow). Horizontal flow is assumed to originate from a point defined by a constant fresh head and a constant salt-water interface height and proceeds toward a hypothetical drain (river) location. The fresh water flow field is assumed to be affected by the rise of the salt-water interface. The solution of the model produces a profile of the interface in the case of stable upconing or, if unstable, the model shows that the interface breaks through to the bottom of the river. In the case of unstable upconing, salt water is being fed directly to the river system from the salt-water reservoir.

Theory

The theory of this model is based upon the work of Hubbert (1940) in which he shows that the angle Θ (Figure III-6) of the interface above the horizontal datum is related to the relative velocities of the two fluids separated by the interface:

$$\text{III-26} \qquad \sin\Theta \approx \frac{\partial Z}{\partial s} = (\gamma_1-\gamma_2)^{-1}\left[\gamma_1 \frac{\partial h_1}{\partial s} - \gamma_2 \frac{\partial h_2}{\partial s}\right]$$

where Z is the elevation of the interface, s is the distance along the interface, γ_1 and γ_2 are the specific weights of the fresh and salt waters, and h_1 and h_2 are the hydraulic heads in the fresh- and salt-water layers. In

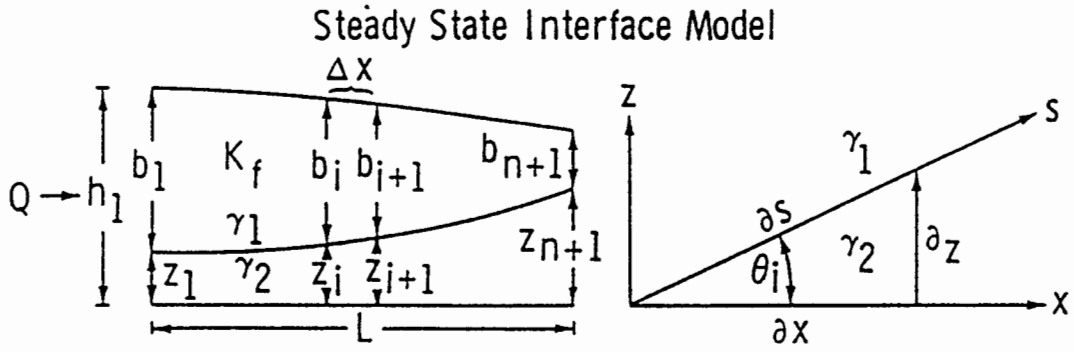

$$\left(\frac{\partial h}{\partial x}\right)_i = -\frac{Q_i}{K_f b_i} \qquad \tan\theta_i = \frac{\gamma_1}{\gamma_1 - \gamma_2}\left(\frac{\partial h}{\partial x}\right)_i$$

$$h_{i+1} = h_i + \left(\frac{\partial h}{\partial x}\right)_i \Delta x \qquad z_{i+1} = z_i + \tan\theta_i \Delta x \qquad b_{i+1} = h_{i+1} - z_{i+1}$$

Figure III-6. Definition diagrams for the free surface-salt water interface upconing model

general both fresh and salt waters are in motion. Application of the chain rule to the derivatives of h_1 and h_2 yields:

$$\text{III-27} \qquad \sin \Theta = (\gamma_1-\gamma_2)^{-1} \left[\gamma_1 \frac{\partial h_1}{\partial x} \bullet \frac{\partial x}{\partial s} - \gamma_2 \frac{\partial h_2}{\partial x} \bullet \frac{\partial x}{\partial x}\right]$$

Observing from Figure III-6 that $\frac{\partial x}{\partial s} \simeq \cos \Theta$ and dividing out this factor yields:

$$\text{III-28} \qquad \tan \Theta = \frac{\sin \Theta}{\cos \Theta} = \frac{\partial z}{\partial s} \bullet \frac{\partial s}{\partial x} = (\gamma_1-\gamma_2)^{-1} \left[\gamma_1 \frac{\partial h_1}{\partial x} - \gamma_2 \frac{\partial h_2}{\partial x}\right]$$

At this point, a static salt water condition is assumed that implies that $\frac{\partial h_2}{\partial x} = 0$ and that

$$\text{III-29} \qquad \tan \Theta \simeq (\gamma_1-\gamma_2)^{-1} \left[\gamma_1 \frac{\partial h_1}{\partial x}\right]$$

This is an excellent assumption when the system is in steady state.

Referring to Figure III-6, it is seen that at any point the flow of the fresh water is defined by

$$\text{III-30} \qquad Q = -K_f b \frac{\partial h}{\partial x}$$

where Q = the discharge per unit width of aquifer,

K_f = the fresh-water hydraulic conductivity,

b = the thickness of aquifer bounded by a salt-water interface and free surface, and

$\frac{\partial h}{\partial x}$ = the hydraulic gradient

Re-arranging equation III-30 yields:

III-31 $$\frac{\partial h}{\partial x} = - \frac{Q}{K_f b}$$

and finally, after substituting equation III-31 into equation III-29,

III-32 $$\tan \Theta = \frac{\gamma_1}{\gamma_2 - \gamma_1} \left(\frac{Q}{K_f b}\right)$$

Numerical Procedure

The model operates by projecting forward in space the positions of the free surface and the interface from the i^{th} node to the $i+1^{th}$ node. The total number of nodes is $(L/\Delta x) + 1$, where L is the distance from a hypothetical constant head boundary to a hypothetical drain (which, if a real stream, would also constitute a constant head if seasonal fluctuations are not considered). The method of projection is simply:

III-33 $$h_{i+1} = h_i + \left(\frac{\partial h}{\partial x}\right)_i \Delta x \qquad , \left(\frac{\partial h}{\partial x}\right)_i = - \frac{Q_i}{K_f b_i}$$

III-34 $$Z_{i+1} = Z_i + \tan \Theta_i \, \Delta x, \quad \tan \Theta_i = \frac{\gamma_1}{\gamma_1 - \gamma_2} \left(\frac{\partial h}{\partial x}\right)_i$$

III-35 $$b_{i+1} = h_{i+1} - Z_{i+1}$$

where h denotes the height of the free surface, Z denotes the height of the interface, and Δx is the node spacing.

Computations proceed from node 1, where h^1, Z^1, b_1, Q, K_f, γ_1, and γ_2 are all known quantities, and move forward toward the n+1 node (see Fig. III-6). Q_i in equation III-33 is the amount of fresh water flowing toward the river at

node i. If R is the recharge (units of length over time), then Q_i is given by

III-36 $$Q_i = R\ell(i-1)\Delta x$$

where ℓ is a unit length transverse to the cross-sectional model. At the river the gain per unit length of stream is

III-37 $$Q/\ell = RL$$

Since the forward projection scheme depends principally upon the accuracy of the estimation of $(\frac{\partial h}{\partial x})_i$, choice of Δx is a crucial factor in achieving the desired degree of accuracy. It is obvious that the value of Δx becomes more important as the discharge point ($n+1^{th}$ node) is approached, since Θ is increasing and tan Θ is also increasing.

Analytical Considerations

The differential equation describing one-dimensional steady-state unconfined flow is

III-38 $$\frac{d}{dx}\left(K_f h \frac{dh}{dx}\right) + R = 0$$

where K_f is the hydraulic conductivity, h is the hydraulic head, and R is the recharge in units of length over time. In this formula h is measured from a zero datum at the base of the unconfined flow. In the case of an interface, h would be measured from the interface. The general solution to equation III-38 is

III-39 $$h^2 = -\frac{R}{K_f} x^2 + C_1 x + C_2$$

where C_1 and C_2 are constants to be determined from the boundary conditions. It has been assumed that K_f, the hydraulic conductivity, is constant. At x=0 we assume a barrier boundary.

III-40 $$h \frac{dh}{dx} = 0 \qquad \text{at } x=0$$

This would correspond to the valley wall or a groundwater divide. This condition implies that $C_1=0$ in equation III-39. Assume that the river is located at x=L. The river's gain per unit length is given by equation III-37. C_2 is simply the head at x=0, denoted by h_o.

III-41 $$h^2 = -\frac{R}{K_f} x^2 + h_o^2$$

This equation assumes a flat interface and was used only to check the numerical procedure and to select an appropriate Δx. It appears that 41 node points give an acceptable accuracy. The error as indicated by comparing the numerical procedure and equation III-41 is less than 2%.

Results

The purpose of this section is to see if stable or unstable upconing occurs in the Smoky Hill River Valley. As shown in Figure III-4, the range of densities for the salt water at the base of the alluvium and in the Wellington Aquifer ranges from 1.0 - 1.2 gm/cm^3. As discussed earlier, L is taken as 9240 feet (half the average valley width) and R is assumed to be .00197 ft/day. K_f ranging from 50-300 ft/day is used. The parameters L, R, and K_f are not precisely known and must be considered average values. For this reason, it would be advisable to let them vary over some range. The other

Table III-2a. Stability table for a range of physical parameters.

$\gamma_2 = 1.05$ gm/cm^3, $K_f = 50$ ft/day

L = 9240 ft., R = .00197 ft/day

$Q/\ell = C = 18.2$ ft^2/day, n = 40

	b_{n+1}					
b_1	L*2 R/2 Q/ℓ=C	L*1.5 R/1.5 Q/ℓ=C	L R Q/ℓ=C	L/1.5 R*1.5 Q/ℓ=C	L/2 R*2 Q/ℓ=C	L R/2 Q/ℓ=C/2
210	unstable	unstable	unstable	unstable	91.9	91.9
200	unstable	unstable	unstable	unstable	67.3	67.3
190	unstable	unstable	unstable	unstable	32.9	32.9
180	unstable	unstable	unstable	unstable	unstable	unstable
170	unstable	unstable	unstable	unstable	unstable	unstable
160	unstable	unstable	unstable	unstable	unstable	unstable
150	unstable	unstable	unstable	unstable	unstable	unstable
140	unstable	unstable	unstable	unstable	unstable	unstable
130	unstable	unstable	unstable	unstable	unstable	unstable

Table III-2b. Stability table for a range of physical parameters.

$\gamma_2 = 1.10$ gm/cm^3, $K_f = 50$ ft/day

L = 9240 ft., R = .00197 ft/day

$Q/\ell = C = 18.2$ ft^2/day, n = 40

	b_{n+1}					
b_1	L*2 R/2 Q/ℓ=C	L*1.5 R/1.5 Q/ℓ=C	L R Q/ℓ=C	L/1.5 R*1.5 Q/ℓ=C	L/2 R*2 Q/ℓ=C	L R/2 Q/ℓ=C/2
210	unstable	unstable	82.6	137.9	158.8	158.8
200	unstable	unstable	54.8	122.2	145.4	145.4
190	unstable	unstable	8.0	105.3	131.4	131.4
180	unstable	unstable	unstable	86.3	116.5	116.5
170	unstable	unstable	unstable	63.8	100.6	100.6
160	unstable	unstable	unstable	32.7	82.8	82.8
150	unstable	unstable	unstable	unstable	62.0	62.0
140	unstable	unstable	unstable	unstable	33.8	33.8
130	unstable	unstable	unstable	unstable	unstable	unstable

Table III-2c. Stability table for a range of physical parameters.

$\gamma_2 = 1.15$ gm/cm^3, $K_f = 50$ ft/day

$L = 9240$ ft., $R = .00197$ ft/day

$Q/\ell = C = 18.2$ ft^2/day, $n = 40$

	b_{n+1}					
b_1	L*2 R/2 Q/ℓ=C	L*1.5 R/1.5 Q/ℓ=C	L R Q/ℓ=C	L/1.5 R*1.5 Q/ℓ=C	L/2 R*2 Q/ℓ=C	L R/2 Q/ℓ=C/2
210	unstable	72.4	133.7	163.0	175.9	175.9
200	unstable	39.5	117.5	150.0	163.8	163.8
190	unstable	unstable	99.8	136.3	151.4	151.4
180	unstable	unstable	79.8	122.1	138.7	138.7
170	unstable	unstable	55.0	106.9	125.5	125.5
160	unstable	unstable	16.0	90.3	111.7	111.7
150	unstable	unstable	unstable	71.5	96.9	96.9
140	unstable	unstable	unstable	48.3	80.7	80.7
130	unstable	unstable	unstable	9.0	62.1	62.1
120	unstable	unstable	unstable	unstable	38.3	38.3
110	unstable	unstable	unstable	unstable	unstable	unstable
100	unstable	unstable	unstable	unstable	unstable	unstable

Table III-2d. Stability table for a range of physical parameters.

$\gamma_2 = 1.20\ gm/cm^3$, $K_f = 50$ ft/day

L = 9240 ft., R = .00197 ft/day

$Q/\ell = C = 18.2\ ft^2/day$, n = 40

	b_{n+1}					
b_1	L*2 R/2 Q/ℓ=C	L*1.5 R/1.5 Q/ℓ=C	L R Q/ℓ=C	L/1.5 R*1.5 Q/ℓ=C	L/2 R*2 Q/ℓ=C	L R/2 Q/ℓ=C/2
210	60.8	115.8	153.4	174.2	183.8	183.8
200	19.0	96.8	139.4			
190	unstable	74.9	124.8	149.6	160.6	160.6
180	unstable	46.5	109.1			
170	unstable	unstable	91.9	123.2	136.4	136.4
160	unstable	unstable	72.2			
150	unstable	unstable	47.5	93.9	110.5	110.5
140	unstable	unstable	3.3			
130	unstable	unstable	unstable	57.6	81.5	81.5
120	unstable	unstable	unstable	31.0		
110	unstable	unstable	unstable	unstable	44.0	44.0
100	unstable	unstable	unstable	unstable	9.5	9.5
90	unstable	unstable	unstable	unstable	unstable	unstable

Table III-2e. Stability table for a range of physical parameters.

K_f = 300 ft/day

L = 9240 feet , R = .00197 ft/day

$Q/\ell = C = 18.2\ ft^2/day$, n = 40

	b_{n+1}			
	γ_2 = 1.05 gm/cm^3		γ_2 = 1.10 gm/cm^3	
	L	L/2	L	L/2
	R	R*2	R	R*2
b_1	Q/ℓ=C	Q/ℓ=C	Q/ℓ=C	Q/ℓ=C
130	70.5	104.3	103.0	117.2
120	----	-----	-----	-----
110	20.4	78.1	76.3	94.6
100	Unstable	-----	-----	-----
90	Unstable	46.2	43.2	70.4
80	Unstable	22.6	16.4	-----
70	Unstable	Unstable	Unstable	42.0
60	Unstable	Unstable	Unstable	-----
55	Unstable	Unstable	Unstable	3.4
50	Unstable	Unstable	Unstable	Unstable

------- = Uncalculated values

Table III-2f. Stability table for a range of physical parameters.

K_f = 300 ft/day

L = 9240 feet , R = .00197 ft/day

$Q/\ell = C = 18.2\ ft^2/day$, n = 40

	b_{n+1}			
	$\gamma_2 = 1.15\ gm/cm^3$		$\gamma_2 = 1.20\ gm/cm^3$	
	L	L/2	L	L/2
	R	R*2	R	R*2
b_1	$Q/\ell=C$	$Q/\ell=C$	$Q/\ell=C$	$Q/\ell=C$
100	74.9	88.3	-----	91.0
90	-----	-----	-----	-----
80	45.2	64.8	-----	68.4
70	24.1	-----	38.6	-----
60	Unstable	37.6	15.5	43.4
50	Unstable	18.4	Unstable	28.2
40	Unstable	Unstable	Unstable	Unstable

----- = Uncalculated values

parameter that has an important influence on whether one has stable or unstable upconing is b_1, the initial saturated thickness of fresh water. Tables III-2a through III-2f show the effect of various combinations of these parameters. These tables clearly show that unstable upconing must be occurring in the Smoky Hill River Valley. For the most dense, and consequently the most stable water (γ_2 = 1.2 gm/cm^3), Table III-2d shows that the initial fresh saturated thickness must be greater than about 90 feet for stable upconing for K_f = 50 ft/day. The most stable situation occurs for γ_2 = 1.2 gm/cm^3 and K_f = 300 ft/day in Table III-2f. However, even in this most optimistic case, the initial fresh saturated thickness must be greater than about 50 feet for stable upconing. Figure III-3, which is a map of the alluvial saturated thickness, shows that between Salina and Solomon the saturated thickness is in the range of 35-50 feet.

The steady-state interface cross-sectional model clearly shows that unstable upconing must be occurring between Salina and Solomon in the Smoky Hill River. The amount of salt water reaching the stream and its response to variations in the water table cannot be found with this model. To answer these questions, a more general time-varying model must be applied.

TIME-VARYING INTERFACE CROSS-SECTIONAL MODEL

Introduction

The work of the previous section dealt with the steady-state position of the interface and assumed a static body of salt water underlying the fresh water. In this section we shall use a model that removes these assumptions. In particular, we shall deal with the time-varying case where the free surface, the interface, the river stage, and the water fluxes (both salt and fresh) can vary with time. The two main approximations that remain in this

model assume a sharp interface and Z averaging in both the fresh- and salt-water layers.

The sharp interface assumes there is an abrupt transition between fresh- and salt-water layers with no hydrodynamic dispersion. The work of the previous section indicates that unstable upconing is to be expected in the Smoky Hill River Valley. In the case of unstable upconing it is not expected that hydrodynamic dispersion is the dominant mechanism for feeding salt water to the river. Hydrodynamic dispersion would have to be the dominant mechanism if stable upconing was occurring some depth below the river (Schmorak and Mercado, 1969). Undoubtedly hydrodynamic dispersion is occurring, but it should be a secondary effect in the presence of unstable upconing.

The Z averaging in both the fresh and salt layers means that we are assuming horizontal flow with vertical equipotentials. At first thought this might seem to be an unreasonable assumption. However, in this and most groundwater models, the lateral extent is so much greater than the vertical dimensions that the slopes of water tables and interfaces rarely exceed 2°. Nevertheless, it is true that the detailed convergence of flow at the river cannot be described with this model. Removing this assumption could be the goal of a more detailed study; however, it is not expected that the qualitative results of this study would be changed.

Theory

Figure III-7 presents the physical situation to be described with model equations. After applying Darcy's Law, the continuity equation, and vertical averaging Bear (1979) obtains

$$\frac{\partial}{\partial x} \bullet \left[(Z_2 - Z_1) \, K_f \frac{\partial h_f}{\partial x} \right] + R_f = S_y \frac{\partial (Z_2 - Z_1)}{\partial t} \qquad \text{III-42}$$

III-43 $$\frac{\partial}{\partial X} \bullet \left[(Z_1 - Z_0)\, K_S \frac{\partial h_S}{\partial X} \right] + R_S = S_y \frac{\partial Z_1}{\partial t}$$

III-44 $$h_S = (Z_1 + \delta Z_2)/(1+\delta)$$

III-45 $$\delta = \gamma_f/(\gamma_S - \gamma_f)$$

III-46 $$h_f = Z_2$$

III-47 $$K_S = K_f(\gamma_S/\gamma_f)$$

where h_f and h_S are the fresh- and salt-water heads; Z_2, Z_1, and Z_0 are the elevations of the water table, interface, and the bedrock; γ_f and γ_S are the specific weights of the fresh and salt water, K_f and K_S are the hydraulic conductivities of the fresh and salt water; S_y is the specific yield; t is the time; R_f and R_S are the fresh- and salt-water recharge; and X is the usual Cartesian coordinate.

Inspection of equations III-42 through III-47 reveals why the sharp interface problem is more difficult to solve than the usual groundwater problem given by equation I-1. Here we have two equations (III-42 and III-43) which must be solved simultaneously. By substitution of equations III-44 and III-46 into equations III-42 and III-43, h_f and h_S can be eliminated from the problem. At this point the two quantities for which we must solve III-42 and III-43 are Z_2 and Z_1, the height of the water table and the interface respectively. Since we have two unknowns, we must have two equations. This is in contrast to equation I-1 which has only one unknown, h.

Numerical Procedure

The same basic techniques used in the solution of I-1 can be used for the solution of equations III-42 and III-43. As always, the initial position for Z_2 and Z_1 must be known and appropriate boundary conditions must be applied at the edge of the model. Finite difference techniques are used to approximate the derivatives in equations III-42 and III-43. This means that a grid of node points with spacing ΔX must be set up just as in the steady-state interface model. However, since we are going to watch things change in time, we must also discretize time into time steps of length Δt.

We have developed two computer programs for the solution of equations III-42 and III-43. One program uses the explicit method (Carnahan and others, 1969) and the other uses the Crank-Nicolson method (Carnahan and others, 1969). Since only one analytical solution to a simple sharp-interface problem is known to us (Shamir and Dagan, 1971), it is difficult to know if the programs are working correctly. However, we are confident the programs are correct for two reasons. First, the steady-state results of the previous section can be reproduced by the time-varying programs. Second, the programs were written independently using entirely different solution techniques. Therefore, if they give the same answers this is strong evidence that the programs are working correctly. Indeed they do give the same results for a number of situations we have investigated.

Application to the Smoky Hill River Valley

Many of the parameters needed for this model have been discussed and used in previous sections. A brief review may be in order. The average fresh-water recharge (R_f) was calculated earlier to be about .00197 ft/day. The average valley width was taken to be about 3.5 miles. This makes the average

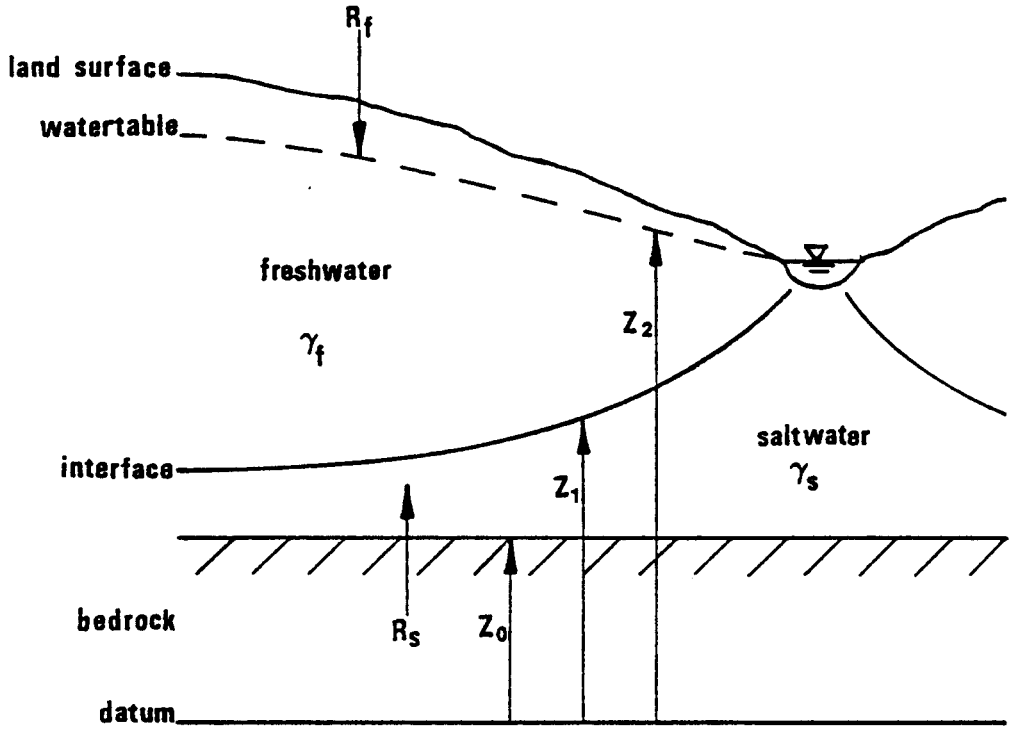

Figure III-7. Sketch of saltwater interface problem.

half width (L) equal to 9240 feet. In the section on the steady-state interface model we chose 41 node points over the distance L with spacing of 231 feet. The first node point was the edge of the model and the 41^{st} node was the river location. This same node arrangement is used for the time-varying model except we use a total of 81 nodes because we are modeling both sides of the river. This is actually done only as a convenience in the modeling; the same data are used on each side of the river so the solution is symmetric about the river. For this reason profiles will be shown only on one side of the river. The average gain of the river per unit length Q/ℓ was previously estimated at 36.4 ft^2/day and will remain the same here. We know from data presented in Figure III-4 that the density of salt water ranges from 1.01 - 1.2 gm/cm^3 in this area. However, we also know that as the density decreases the upconing becomes more unstable. In this model we shall usually take the density of salt water to be 1.2 gm/cm^3 (which is the most stable case); however, just to check the effect of density, 1.1 has been used for some runs that will be mentioned later.

Gillespie and Hargadine (1980) state that brine discharge between 1974 and 1977 ranged from 1.77 ft^3/sec to .31 ft^3/sec with an average of .77 ft^3/sec. They also state that the 50% exceeded flow at New Cambria is 110 ft^3/sec. When this is added to the 15.6 ft^3/sec gain measured by Gillespie and Hargadine between New Cambria and Solomon we find the average river flow to be about 126 ft^3/sec. If the .77 ft^3/sec of brine is near saturation at 180,000 ppm the resulting river concentration of chloride would be

$$\frac{.77}{126} \times 180{,}000 \text{ ppm} = 1100 \text{ ppm}$$

We need to know the salt-water flux per unit area (R_S) from the Wellington

aquifer into the alluvial aquifer. Using the same procedures and dimensions as used in calculating the fresh-water recharge on page 38, we obtain

$$R_S = \frac{.77 \text{ ft}^3/\text{sec}}{(7\text{x}5280 \text{ ft})(3.5\text{x}5280 \text{ ft})} = .0000974 \text{ ft/day}$$

This is the average flux of salt water per unit area entering the alluvial aquifer. For lack of better information, we assume the flux is uniform over the whole intrusion area.

Figure III-8 shows a cross section of the Smoky Hill River Valley and its location. This cross-sectional data was taken from the digitized data used in the Wellington aquifer model study. Notice that the average saturated thickness away from the river is about 40 feet. Also notice that the water table is 8-13 feet higher than the river when one is 10,000 feet or more away from the river.

For our initial run of the time-varying model we chose K_f equal to 300 ft/day and S_y equal to .15 (S_y is the specific yield and varies from .15 - .18 for typical Kansas alluvial aquifers). The boundary conditions that we chose for the model required the water table and the interface to be flat at the edge of the model. From Figure III-8 we chose 40 feet of saturated thickness near the edge of the model. Given the salt-water flux, we allowed the model to run for a salt-water density of 1.2 gm/cm^3 and found that unstable upconing occurred under the river. This, of course, was expected from the steady state work.

At this point, it was necessary to restrict the rise of salt-water under the river. Physically, it is obvious that the interface must always be below the water table. However, mathematically, the model only sees that unstable upconing is occurring and allows the interface to continue to rise. When the

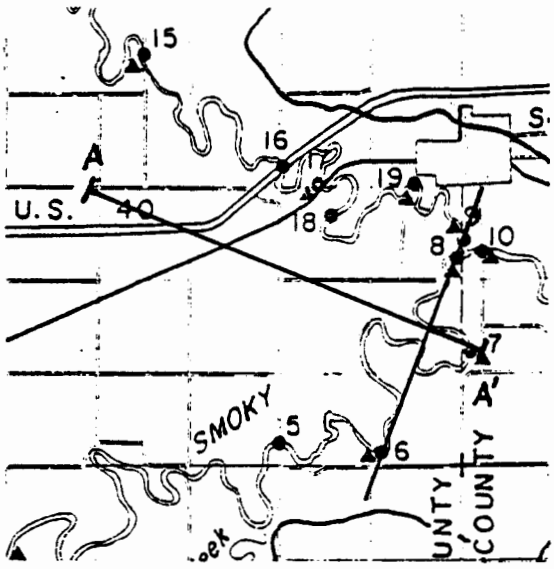

(From Gillespie and Hargadine, 1980)

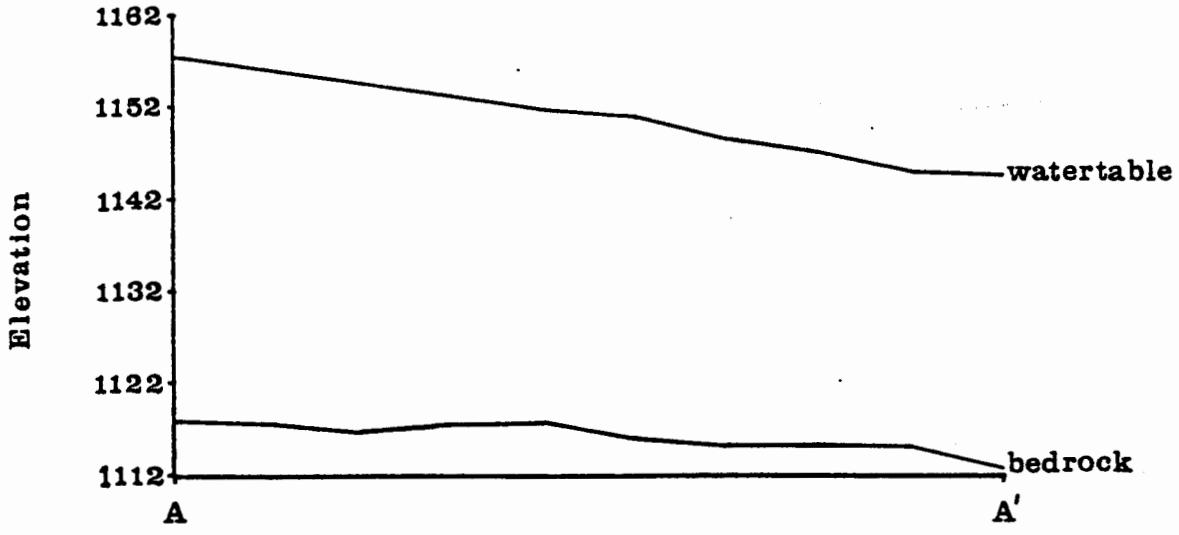

Figure III-8. Alluvial aquifer cross-section A-A' and its location.

interface exceeds the water table, the model gives absurd answers. What must happen, of course, is that the sink of water (in this case the river) must carry away the salt water and prevent the interface from rising beyond a certain point. As mentioned earlier this model is averaged in the Z direction and cannot describe in detail what happens at the river. For these reasons, we decided to only allow the interface to come within 10 feet of the watertable at the river. In other words, at this height we assume the cone intercepts the river bottom and the salt water is carried away by the river.

Results

By restricting the rise of salt water under the river, we can let the model run to steady state and see what the interface looks like. Figure III-9 shows this steady-state interface. Notice that if one is more than eight nodes away from the river, the salt-water layer is less than 2 feet thick. The drawdown at the river is about 10 feet. The interface seems to slope away from the river rapidly but one must remember the vertical exaggeration. In fact, the slope of the interface is always less than 2^{o}.

The model results shown in Figure III-9 are for K_f equal to 300 ft/day. We also tried smaller values of K_f. We found that a K_f less than about 150 ft/day just did not work; the drawdown at the river was much too great. In fact, the drawdown at the river for K_f of 150 ft/day was about 20 feet, which is probably too large. A K_f of 200 ft/day produces a drawdown at the river of about 14 feet. The conclusion is that K_f is probably in the range of 200-300 ft/day.

We also tested the effect of varying other parameters. For example, changing the density of salt water to 1.1 gm/cm^3 produced results very close (drawdown at river changed only .65 feet) to those presented in Figure III-

9. We also tried doubling L and halving R_f and R_s so that the total flux of fresh and salt water remained the same. The results produced were almost identical to the K_f equal to 150 ft/day case mentioned above. The drawdown at the river was about 20 feet, which is probably too much.

At this point, we feel we have a good model, with K_f equal to 300 ft/day and L equal to 9240 feet. It appears that the model results are not too sensitive to the salt water density used, since unstable upconing occurs even for the heaviest water.

The steady-state situation depicted in Figure III-9 results in about 1.8 ft^3 of saltwater intrusion to the river per day per unit length.

$$Q_s/\ell = 1.8 \text{ ft}^2/\text{day}$$

The question arises as to how this saltwater intrusion reacts to a typical flood event. Figure III-10 is taken from Gillespie and Hargadine (1980); it shows the river stage and chloride discharge for the years 1973 through 1977. In general, it is seen that the chloride discharge goes down when the river stage rises. Does our model predict this behavior? Notice the flood event that took place from April to July in 1974. In about a two month period during April and May the river stage rose about 5 feet. Notice that the chloride discharge declines steadily during this period and reaches its lowest value when the river stage is at its highest value. For the next two months the river stage falls rather uniformly and the chloride discharge increases. At the end of about four months, the river is again in a baseflow condition and the chloride discharge is at a high value. Over the next few months the chloride discharge decays to a more normal value.

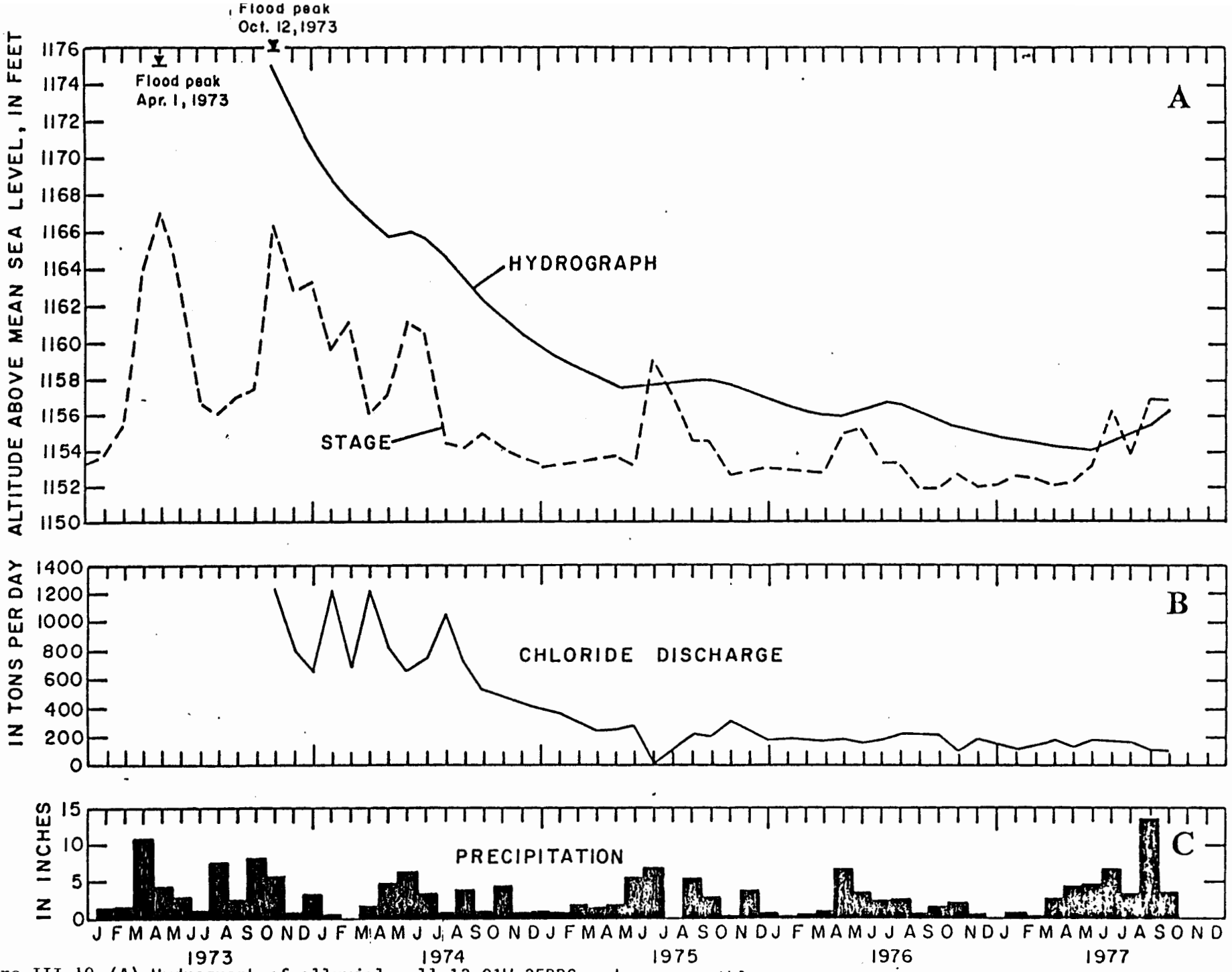

Figure III-10. (A) Hydrograph of alluvial well 13-01W-35BBC and mean monthly stage in the Smoky Hill River near the well, (B) mean monthly chloride discharge to the Smoky Hill and Solomon Rivers from New Cambria to Enterprise, and (C) monthly precipitation at Salina.

(From Gillespie and Hargadine, 1980)

The dashed line in Figure III-11 represents a hypothetical flood event with essentially the same character as the real one just discussed. This time varying river stage can be placed in our sharp-interface model. The response of the salt-water intrusion flux per unit length of river is shown by the solid curve for K_f of 300 ft/day, salt-water density of 1.2 gm/cm^3, and L equal to 9240 feet. Notice that the salt-water intrusion drops dramatically while the river stage is rising. In fact the flux shown in Figure III-11 goes negative. This does not mean that salt water suddenly is fed from the river to the alluvial aquifer (although this could occur on a small scale). The negative flux at the river simply means that temporarily unstable upconing has stopped and the salt-water mound under the river is temporarily declining. However, observe that as the river stage declines the unstable upconing reoccurs and causes the maximum salt-water flux to occur when the river has reached its baseflow condition again. From this point on the salt-water intrusion decays slowly back to the normal value of 1.8 ft^2/day over a period of about 2-3 months. This behavior is actually quite logical when one recalls that the amount of upconing is related to the groundwater discharge to the river. During the rising river stage the river is feeding the groundwater system and the salt-water intrusion or unstable upconing is shut off. During the falling river stage, bank storage causes the groundwater discharge to be greater than normal causing greater than normal salt-water intrusion.

Note that in the real world the river chloride discharge rarely goes to zero. This is because there are other sources of chloride upstream from this area. Also several bigger flood events previous to the one we have considered complicate the interpretation. However, notice that between June and July of 1975 the chloride discharge does drop almost to zero in response to a flood event.

We have produced flood-event responses for a number of different values for K_f, γ_s, and L. Generally the only effect is to change the height of the peaks in Figure III-11. Qualitatively the response is the same. For example, reducing the hydraulic conductivity K_f lowers the maximum salt-water intrusion at 120 days. It is 10.9 ft^2/day for K_f of 300 ft/day, 9.2 ft^2/day for K_f of 200 ft/day, and 6.9 ft^2/day for K_f of 150 ft/day. Decreasing the density of salt water to 1.1 gm/cm^3 makes the upconing more unstable and increases the maximum salt-water intrusion at 120 days to 11.7 ft^2/day. Doubling L and halving R_f and R_s lowers the maximum salt-water flux at 120 days to 8.2 ft^2/day.

At this point, it is clear that the unstable upconing mechanism can account qualitatively for the response of the chloride discharge to a flood event. It is more difficult to make quantitative predictions due to our lack of detailed data. The data from Gillespie and Hargadine (1980) in Figure III-12 show a river discharge of about 600 ft^3/sec just after the flood event of 1974 in July and August. At about this time, the chloride concentration in the river obtains its peak value of nearly 1000 mg/ℓ. Depending on whether we use a salt-water density of 1.2 or 1.1, the model predicts a maximum salt-water flux of 4.7 ft^3/sec or 5.0 ft^3/sec for the reach from New Cambria to Solomon. From Figure III-4 we see that salt water with a density of 1.2 gm/cm^3 corresponds to about 180,000 mg/ℓ chloride and 1.1 gm/cm^3 corresponds to about 90,000 mg/ℓ. Converting these figures to river concentrations gives

$$\frac{4.7\ ft^3/sec}{600\ ft^3/sec} \times 180{,}000\ mg/\ell = 1410\ mg/\ell$$

$$\frac{5.0\ ft^3/sec}{600\ ft^3/sec} \times 90{,}000\ mg/\ell = 750\ mg/\ell$$

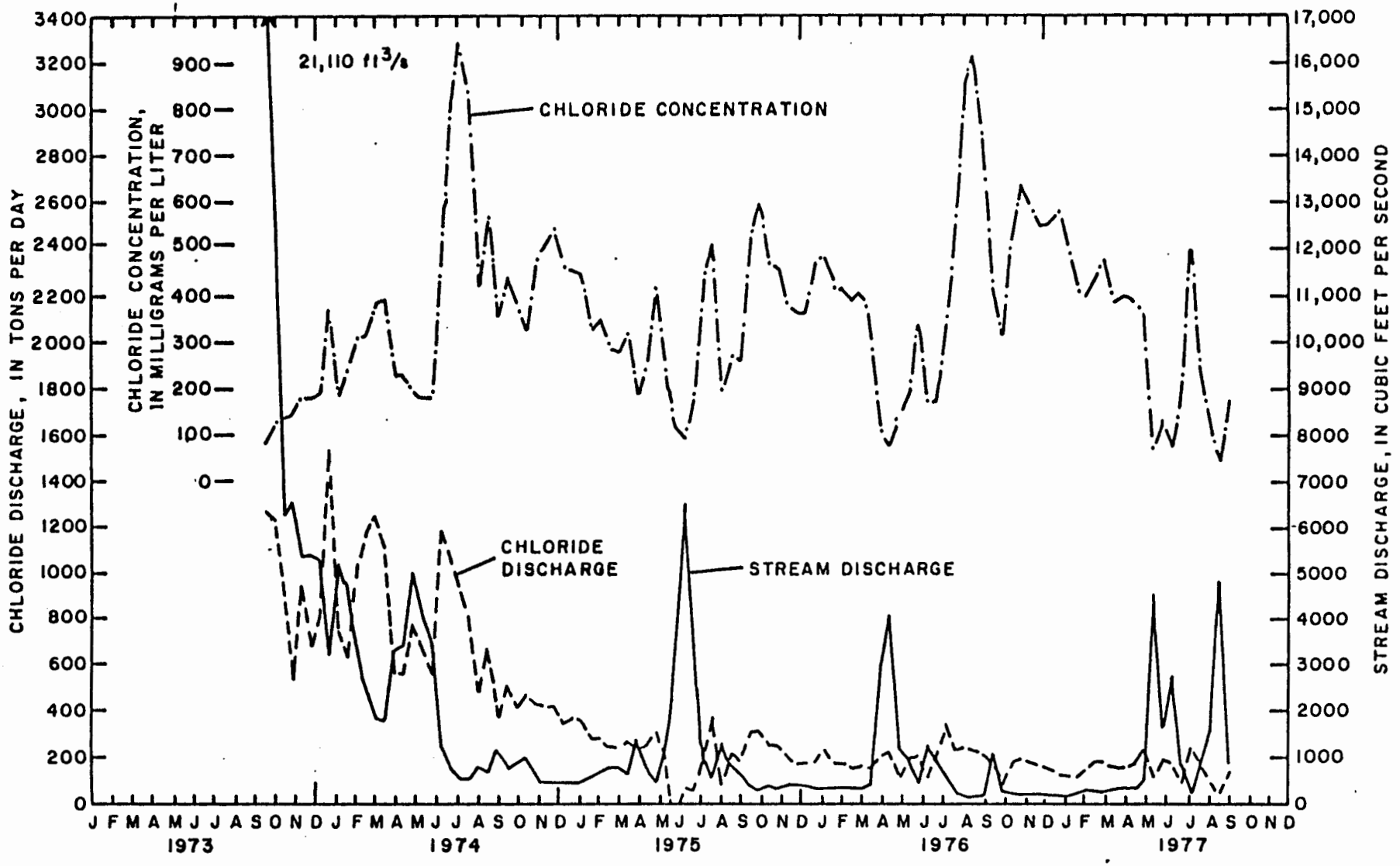

Figure III-12. (A) Mean biweekly chloride discharge to the Smoky Hill and Solomon Rivers from New Cambria to Enterprise, (B) mean biweekly streamflow discharge in the Smoky Hill River at Enterprise, and (C) mean biweekly chloride concentrations in the Smoky Hill River at Enterprise.

(From Gillespie and Hargadine, 1980)

Since the background river concentration for this time period is given by Gillespie and Hargadine (1980) as about 200-300 mg/ℓ chloride, it would appear that salt water of density 1.1 gm/cm^3 would give the measured peak chloride concentration of about 1000 mg/ℓ. The prediction using saltwater of 1.2 gm/cm^3 would be about 50 to 60% too high.

From the model study of the Wellington aquifer, it is clear that a reduction in the salt-water flux from the Wellington aquifer to the alluvial aquifer by a relief-well system will be less than 25%. We have reduced R_s by 25% and run the model to a new steady-state solution. The results for K_f of 300 ft/day and a salt-water density of 1.2 gm/cm^3 are shown in Figure III-13. About half of the reduction or 12.5% is experienced in the river during the first 1500 days (slightly more than 4 years). About 80% of the ultimate 25% reduction (20%) in salt-water flux to the river is achieved in about 3900 days or about 10.7 years. The additional 5% reduction occurs slowly over the next several years. Of course, these are <u>average</u> reductions. As we have seen earlier, flood events can cause the chloride discharge to vary considerably over the range of several months. We have just discussed a 25% reduction in salt-water flux to the alluvial aquifer from the Wellington aquifer; however, any reduction follows this same curve. For example, a 12.5% reduction is shown on the right hand scale in Figure III-13. This has been verified by model runs.

Varying K_f and the density of the salt water have very little effect on the data presented in Figure III-13. However, doubling L while halving R_f and R_s does modify the results considerably. The net effect is that the time

Figure III-13. Response of saltwater intrusion to a 25% or 12.50% reduction of saltwater flux into the alluvial aquifer.

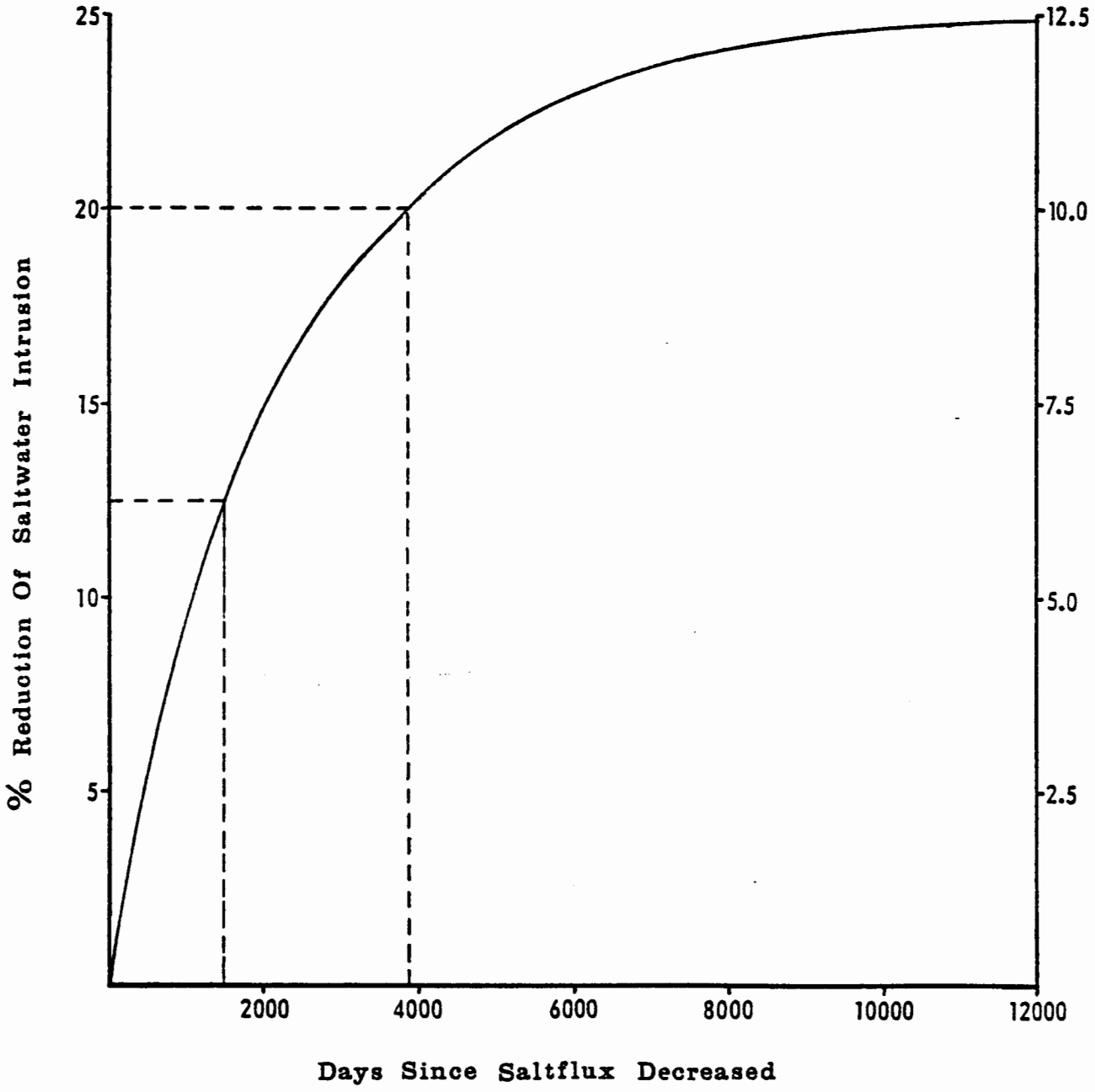

One could pump into the reservoir when the river chloride was too high and pump directly into the river when the river chloride was low. Modeling of such a system is a possible extension of this investigation.

With regard to additional data that might be collected, the following comments are offered. Additional resistivity data would be very useful if it can find the salt-water layer. In particular, it could confirm or refute upconing in a particular area. Alternatively, it might be able to find collapse or sink features that lead to a salt-water plume or interface due to increased hydraulic conductivity of the confining layer. Drilling and testing more alluvial wells would better define the water table and would give a better estimate of the alluvial hydraulic conductivity. However, it is not likely this information would significantly change the model results. Multilevel nests of wells could determine the stratification of the water. In particular, wells near the river could be used to confirm or refute upconing in that area. Field determination of water stratification, especially near the river, would seem to be one of the most important pieces of new data that could be developed. In conjunction with this, detailed seepage and salinity analyses might be done to locate areas where salt-water intrusion to the river is consistently dominant. In these areas the detailed work on stratification should be concentrated.

Since the convergence of the groundwater flow lines near the river is responsible for the unstable upconing, an alternative relief well system might be effective. Once those reaches of the stream that were consistently contributing salt water were identified, it might be possible to locate bank-side alluvial wells, screened near the base of the alluvium, which could be pumped to counteract the unstable upconing and to intercept the salt water before it reached the stream. These wells, in conjunction with a surface reservoir, might make it possible to manage the quality of the river water. Eventually all the pumped water would be put into the river; however, the timing could be chosen to prevent the chloride level from rising too high.

scale is doubled in Figure III-13. In other words the 12.5% reduction occurs at 3000 days rather than 1500 days. This is because the lateral extent of the alluvial aquifer has been doubled; therefore, it takes longer for the excess salt water to be flushed out.

CONCLUSIONS

The steady-state models presented in this section indicate that the salt water in the Smoky Hill River Valley should be in an unstable condition near the river. This indicates that unstable upconing should be a dominant mechanism for feeding salt water to the river system. The groundwater system does not uniformly discharge to the river system. The unstable upconing should be most pronounced in those reaches where the groundwater system consistently feeds the river system. These areas could be delineated by seepage and salinity surveys. Some of this work has already been done but much more data are needed.

The time-varying model shows that the response of the chloride discharge to a flood event can be qualitatively explained by the unstable upconing mechanism. In addition, the time varying model shows that several years would elapse before significant benefit would be seen in the river system from a Wellington aquifer relief well scheme.

A more sophisticated model to fully describe three-dimensional effects is a possible extension of this study. This would allow one to drop the sharp interface approximation. It is hard to say how much difference that would make in the model results. Intuitively, it seems that a 3-D model would predict more salt-water flow to the river because an additional mechanism, hydrodynamic dispersion, has been added. One would not expect the salt water to be more stable in a 3-D model.

Appendix I. Well location for various pumping schemes.

6 WELL LOCATION

I	J
7	9
8	9
9	9
10	9
11	9
12	9

20 WELL LOCATION -

SPACING -

2000 ft		4000 ft	
I	J	I	J
7	9	7	9
8	9	8	9
9	9	9	9
10	9	10	9
11	9	11	9
12	9	12	9
6	10	6	11
7	10	7	11
8	10	8	11
9	10	9	11
10	10	10	11
11	10	11	11
12	10	12	11
6	11	6	13
7	11	7	13
8	11	8	13
9	11	9	13
10	11	10	13
11	11	11	13
12	11	12	13

BIBLIOGRAPHY

Bear, Jacob, 1979, Hydraulics of groundwater: McGraw-Hill International Book Company, New York, 567 p.

Bear, J., and Dagan, G., 1964, The unsteady interface below a coastal collector: Hydraulic Lab Prog. Rep. 3, Technion, Haifa, Israel.

Bear, J., and Dagan, G., 1966a, Increasing the yield of a coastal collector by means of special operation techniques: Hydraulic Lab. Prog. Rep. 4, Technion, Haifa, Israel.

Bear, J., and Dagan, G., 1966b, The transition zone at a rising interface below a collector: Hydraulic Lab. Prog. Rep. 5, Technion, Haifa, Israel.

Bear, J., and Dagan, G., 1968, Solving the problem of local interface upconing in a coastal aquifer by the method of small perturbations: J. Hydraul. Res., p. 1.

Carnahan, B., Luther, H.A., and Wilkes, J.O., 1969, Applied numerical methods: John Wiley, New York, 604 p.

Cobb, P.M., McElwee, C.D., and Butt, M.A., 1978, Leaky aquifer parameter identification by sensitivity analysis: Midwestern AGU meeting, St. Louis, Mo., AGU Doc. #E79-002.

Cobb, Patrick, 1980, The distribution and mechanisms of salt water intrusion in the fresh water aquifer and in Rattlesnake Creek, Stafford County, Kansas: Master's Thesis, Dept. of Civil Engineering, The University of Kansas, Lawrence, Kansas.

Freeze, R. Allan, and Cherry, John A., 1979, Groundwater: Prentice-Hall, Inc., Englewood Cliffs, New Jersey, 604 p.

Gogel, Tony, 1979, Discharge of saltwater from permian rocks to major stream-aquifer systems in central and south-central Kansas: USGS Open File Report 79-1055, Lawrence, Kansas. (Now published as KGS Chemical Quality Series 9, 1981.)

Gillespie, J.B., 1979, Results of aquifer tests in the Wellington Aquifer near Salina, Kansas; USGS preliminary report, Lawrence, Kansas.

Gillespie, J.B., 1980, Personal communication: USGS Water Resources Div., Kansas District, Lawrence, Kansas.

Gillespie, J.B., and Hargadine, G.D., 1980, Saline groundwater discharge to the Smoky Hill River between Salina and Abilene, central Kansas: USGS preliminary report, Lawrence, Kansas.

Hubbert, M. King, 1940, The theory of ground-water motion: The Journal of Geology, v. 48, no. 8, pt. 1, p. 785-944. Reprinted and corrected in Hubbert, M. King, 1969, The theory of ground-water motion and related papers: Hafner Publishing Company, New York, p. 25-184.

McWhorter, David B., 1972, Steady and unsteady flow of fresh water in saline aquifers: Colorado State University, Water Management Technical Report No. 20, 49 p.

Mercer, James W., Larson, Steven P., and Faust, Charles R., 1980, Simulation of salt-water interface motion: Groundwater, v. 18, no. 4, p. 374-385.

Muskat, M., 1937, The flow of homogeneous fluids through porous media: McGraw-Hill, New York, 763 p.

Muskat, M., and Wyckoff, R.D., 1935, A.I.M.E., 114, Pet. Dev. Techn. 144.

Schmorak, S., and Mercado, A., 1969, Upconing of fresh water - sea water interface below pumping wells, field study: Water Resources Research, v. 5, no. 6, p. 1290-1311.

Shamir, U., and Dagan, G., 1970, Motion of the sea water interface in a coastal aquifer: Hydraulic Lab., Technion, Haifa.

Shamir, U., and Dagan, G., 1971, Motion of the seawater interface in coastal aquifers: a numerical solution: Water Resources Research, v. 7, no. 3, p. 644-657.

Trescott, P.C., Pinder, G.F., and Larson, S.P., 1976, Finite-difference model for aquifer simulation in two dimensions with results of numerical experiments: Techniques of Water-Resources Investigations of the U.S. Geological Survey, Book 7, Chapter C1.

Verruijt, Arnold, 1980, The rotation of a vertical interface in a porous medium: Water Resources Research, v. 16, no. 1, p. 239-240.